

Analysis and Design of Discrete  
Normals and Curvatures

Torsten Langer Alexander G. Belyaev  
Hans-Peter Seidel

MPI-I-2005-4-003

March 2005

FORSCHUNGSBERICHT RESEARCHREPORT

MAX-PLANCK-INSTITUT  
FÜR  
INFORMATIK

---



## **Authors' Addresses**

Torsten Langer  
Max-Planck-Institut für Informatik  
Stuhlsatzenhausweg 85  
66123 Saarbrücken  
**langer@mpi-sb.mpg.de**

Alexander G. Belyaev  
Max-Planck-Institut für Informatik  
Stuhlsatzenhausweg 85  
66123 Saarbrücken  
**belyaev@mpi-sb.mpg.de**

Hans-Peter Seidel  
Max-Planck-Institut für Informatik  
Stuhlsatzenhausweg 85  
66123 Saarbrücken  
**hpseidel@mpi-sb.mpg.de**

## Abstract

Accurate estimations of geometric properties of a surface (a curve) from its discrete approximation are important for many computer graphics and computer vision applications. To assess and improve the quality of such an approximation we assume that the smooth surface (curve) is known in general form. Then we can represent the surface (curve) by a Taylor series expansion and compare its geometric properties with the corresponding discrete approximations. In turn we can either prove convergence of these approximations towards the true properties as the edge lengths tend to zero, or we can get hints how to eliminate the error. In this report we propose and study discrete schemes for estimating the curvature and torsion of a smooth 3D curve approximated by a polyline. Thereby we make some interesting findings about connections between (smooth) classical curves and certain estimation schemes for polylines. Furthermore, we consider several popular schemes for estimating the surface normal of a dense triangle mesh interpolating a smooth surface, and analyze their asymptotic properties. Special attention is paid to the mean curvature vector, that approximates both, normal direction and mean curvature. We evaluate a common discrete approximation and show how asymptotic analysis can be used to improve it.

It turns out that the integral formulation of the mean curvature

$$H = \frac{1}{2\pi} \int_0^{2\pi} \kappa(\phi) d\phi,$$

can be computed by an exact quadrature formula. The same is true for the integral formulations of Gaussian curvature and the Taubin tensor. The exact quadratures are then used to obtain reliable estimates of the curvature tensor of a smooth surface approximated by a dense triangle mesh. The proposed method is fast and often demonstrates a better performance than conventional curvature tensor estimation approaches. We also show that the curvature tensor approximated by our approach converges towards the true curvature tensor as the edge lengths tend to zero.

## Keywords

Asymptotic Analysis, Polyline, Polygonal Mesh, Curvature, Torsion, Curvature Tensor, Gaussian Curvature, Mean Curvature, Principal Directions

# 1 Introduction

Given a dense triangle mesh approximating a smooth surface, one of the most fundamental problems consists in accurately estimating surface characteristics like normals and curvatures of the mesh. Normals are important by themselves, e.g. for smooth shading [Gou71, Pho75], but robust estimates are even more important for derived properties: curvatures and their derivatives [Tau95a, Rus04, TRZS04].

The mean curvature vector is related to the Laplacian, and its computation is the core of many smoothing and fairing algorithms [Tau95b, DMSB99], Gaussian curvature is a measure of deviation from flatness, and the principal directions can be used for “geometrically meaningful” remeshing [ACSD<sup>+</sup>03]. Mean curvature, Gaussian curvature and principal directions together are often referred to as curvature tensor. It is essential for many more tasks, like mesh segmentation, feature detection and non-photorealistic rendering [DFRS03, OBS04].

One common way to obtain normal vectors at a vertex of a triangle mesh is to compute it as a weighted average of the normals of the incident triangles. Various weights have been proposed for that purpose. Perhaps the most popular schemes are uniform weighting [Gla90], weighting by areas [Tau95a], weighting by inverse areas [HDW98] and spherical weighting as introduced in [Max99] which is exact on spheres. In contrast to the previous methods, Meyer et al. [MDSB02] use a weighted average of the *edges* to get an approximation of not only the normal direction but also the mean curvature.

The first two sections of this paper are devoted to the development of a mathematical apparatus for the asymptotic analysis of curves and surfaces, and applying it to known approximation schemes. A uniform treatment for various approximations of tangents, normals, curvatures, torsions, and further differential properties is given. It allows a rigorous mathematical analysis and comparison of different approaches and can help to improve them. Applications include the evaluation of planar curves [ABS02] and extend to space curves and surfaces. We analyze approximations for the first and second order derivatives of space curves as well as for normal vectors on a mesh. In particular, we show that all known weighting schemes for mesh normals behave asymptotically similar, converging linearly in general and quadratically for a wide class of regular vertices. The mean curvature vector approximation [MDSB02] has to be modified slightly to achieve this result. Even then convergence of the length towards the mean curvature can only be guaranteed for a very limited class of vertices.

Generally, the situation is much more difficult for surface curvatures. The first attempts to define and determine the curvature of a surface date back at least to the eighteenth century when Euler and Gauß laid the foundations for smooth surfaces [Kat98]. Euler [Eul60] recognized the relationship between the principal

curvatures and normal curvatures in arbitrary directions,

$$\kappa(\phi) = \kappa_{\max} \cos^2 \phi + \kappa_{\min} \sin^2 \phi \quad (1)$$

now known as *Euler's formula*, where  $\kappa_{\max}$  and  $\kappa_{\min}$  are the maximal and minimal principal curvatures, respectively,  $\kappa(\phi)$  is the directional curvature corresponding to tangent direction  $\mathbf{t}(\phi)$  and  $\phi$  is the angle between  $\mathbf{t}(\phi)$  and the maximal principal direction.

In the nineteenth century the seminal work of Gauß [Gau27] gave a more general framework for the curvature of surfaces, introducing a local surface quantity measuring how far a surface is from being flat. The quantity received the name *Gaussian curvature*  $K$  and turned out to be one of the most important intrinsic surface characteristics.

A popular discrete approximation estimates the Gaussian curvature at vertex  $P$  of a mesh  $\mathcal{M}$  approximating a smooth surface via the angle deficit at  $P$

$$K \approx \frac{2\pi - \sum_i \alpha_i}{\frac{1}{3}A_{\mathcal{M}}} \quad (2)$$

where  $\alpha_i$  is the angle of the  $i$ -th mesh triangle adjacent to  $P$  and  $A_{\mathcal{M}}$  is the area of the one-ring formed by these triangles. Some modifications of the angle deficit approximation (2) are considered in [MDSB02, MD02] and suggest certain changes of the denominator in (2). Approximation (2) is based on lesser known formulae of Legendre and Gauß [MD02], which deliver asymptotic expansions of the difference between an angle  $\beta_i$  of a geodesic triangle on a surface  $\mathcal{S}$  and the corresponding angle  $\gamma_i$  of the flat triangle whose edges are of equal length as the edges of the geodesic triangle. It can be shown that up to terms quadratic with respect to the edge lengths

$$K = \frac{2\pi - \sum_i \gamma_i}{\frac{1}{3}A_{\mathcal{S}}}$$

where the sum is over all triangles adjacent to  $P$ , and  $A_{\mathcal{S}}$  is the area of the polygon composed of the respective flat triangles. Unfortunately, the convergence of Approximation (2) is only given for rather special conditions [MW00, BCM03]. The reason is that the quadratic error in the numerator (by approximation of  $\gamma_i$ ) and the quadratic term in the denominator (as the area shrinks to zero) yield a total error of  $O(1)$ . The advantage of this formula is that the sum of the Gaussian curvature over all vertices satisfies the global Gauß-Bonnet theorem (a generalization of the angle deficit formula), which is a deep topological result.

Curvature estimation still remains an active research area with many applications. Yet, to compute the complete curvature tensor no such simple formulae as for the Gaussian curvature are known. We will give just a small selection of

recent studies. Goldfeather and Interrante [GI04] presented methods to fit a polynomial to the one-ring of a vertex. Then the exact curvature of the polynomial serves as an estimate of the mesh curvature. Many other approaches use a (more or less) special definition of the curvature tensor from differential geometry and try to find an appropriate discretization [Rus04, TRZS04, MDSB02]. As a special case of these “differential geometry methods” we would like to mention the works of Taubin [Tau95a] and Watanabe and Belyaev [WB01]. They approximate an integral over all angular directions to obtain an expression for the curvature tensor (Taubin) or only the principal curvatures (Watanabe and Belyaev), respectively.

In these cases the correct discretization of the complete integral from a small number of samples in the directions of the edges incident to the central vertex poses a special problem. Taubin suggests area weights (of the triangles incident to the respective edges) while Watanabe and Belyaev use angular weights that give a trapezoidal approximation of the integral. But none of these weights can be expected to give exact results, even if the edge lengths tend to zero. Convergence to the correct value could only be achieved if the number of edges tended to infinity, but this is not a practical assumption.

Based on our asymptotic analysis, we present exact quadratures for the mean curvature

$$H = \frac{1}{2\pi} \int_0^{2\pi} \kappa(\phi) d\phi, \quad (3)$$

Gaussian curvature

$$K = 3H^2 - \frac{1}{\pi} \int_0^{2\pi} \kappa(\phi)^2 d\phi, \quad (4)$$

and the Taubin tensor

$$\mathbf{M} = \frac{1}{2\pi} \int_0^{2\pi} \kappa(\phi) \mathbf{t}(\phi) \mathbf{t}(\phi)^t d\phi. \quad (5)$$

These integrals can be computed exactly from the normal curvatures  $\kappa_i$  along the edges of a mesh. We prove the convergence of our method if approximated values are used to obtain these normal curvatures.

In real world applications all these computations have often to be carried out in the presence of noise. In this paper we assume that all points lie exactly on a smooth surface, since the definitions for differential properties are valid only in that case. Techniques to cope with noisy data can be found in [MN03] and [HS03].

There are basically two ways to evaluate the quality of any of these methods. On the one hand, they can be applied to a specific tessellated analytical surface and the result can be compared with the exact surface normal (or any other approximated geometric property) at the corresponding point [MW00, MDSB02]. On the other hand, an asymptotic analysis can be applied. In this case, the analytical

surface is given in general form, usually represented by a Taylor series expansion. Then the outcome of the discrete approximation can again be compared to the real surface normal. Both methods have advantages and drawbacks. The first one cannot state general results, but only for certain test surfaces. The second method holds for all (analytical) surfaces and can give clues for improvement of the approximations. But it is only helpful for dense meshes where dense is not well-defined. It has successfully been applied for curves [ABS02, Bou00], but for surfaces a comprehensive treatment has not been achieved so far. Pioneering work was done in [MW00, CSM03].

The remainder of this report is organized as follows: in Section 2, we will analyze the convergence behavior of curvature and torsion approximations for space curves, and in Section 3 we will use our method to evaluate normal approximations on meshes. In Section 4 we will present a novel method to gain fast and reliable estimates for mean curvature, Gaussian curvature, and the curvature tensor. We will introduce quadratures to compute certain curvature integrals exactly, given only three different normal curvatures and the angles between the respective geodesics. Furthermore, we will show how the necessary curvatures and angles can be approximated such that a convergence guarantee of our method can be given if the edge lengths tend to zero. An experimental validation will be given in Section 5, and, in Section 6, we will present our conclusions. Three appendices give further details of the mathematical foundations of our proofs.

## 2 Space curves

As shown in [ABS02], the (2-dimensional) Frenet frame of a planar curve can be used to evaluate the discrete estimations of curve normals and curvatures. The same method carries over to the case of space curves using the 3-dimensional Frenet frame. We will show here that the same formulae essentially still hold to compute tangent vectors and curvatures of 3D curves. Additionally, we propose and evaluate an approximation for torsion of a space curve. Due to the nature of torsion, being a third derivative, we need at least 4 points to do this, but we consider also an estimation using 5 points to obtain better results. See also [Bou00] for more estimations.

Let a smooth curve  $\mathbf{r}$  be interpolated by the five points  $P_{-2}, P_{-1}, P_0, P_1,$  and  $P_2$ , with the corresponding edges  $\overrightarrow{P_i P_{i+1}}$  denoted by  $\mathbf{c}, \mathbf{d}, \mathbf{e},$  and  $\mathbf{f}$ , and their lengths denoted by  $c, d, e,$  and  $f$ , see Figure 1. Then those edges can be expressed by their Taylor expansions in the coordinate system given by the Frenet frame of  $\mathbf{r}$  with tangent  $\mathbf{t}$ , normal  $\mathbf{n}$  and binormal  $\mathbf{b} = \mathbf{t} \times \mathbf{n}$ . Let further  $\kappa$  denote the curvature at  $P_0$  and  $\tau$  denote the torsion at the same point. For the exact expansions, refer to Appendix A.

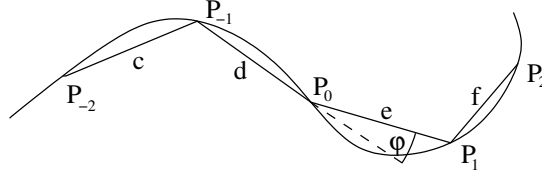


Figure 1: A space curve.

First, we approximate  $\mathbf{r}$  by a circle.

**2.1 Proposition (tangent vector).** *The tangent of the circle passing through  $P_{-1}$ ,  $P_0$  and  $P_1$  is a second order approximation of the real tangent of the curve:*

$$\begin{aligned}
\tilde{\mathbf{t}} &:= \frac{de}{d+e} \left( \frac{\mathbf{d}}{d^2} + \frac{\mathbf{e}}{e^2} \right) \\
&= \mathbf{t} \left( 1 - \frac{de}{8} \kappa^2 + \frac{d^2e - de^2}{12} \kappa \kappa' + O(d, e)^4 \right) \\
&+ \mathbf{n} \left( \frac{de}{6} \kappa' - \frac{d^2e - de^2}{24} (\kappa'' - \kappa \tau^2) + O(d, e)^4 \right) \\
&+ \mathbf{b} \left( -\frac{de}{6} \kappa \tau + \frac{d^2e - de^2}{24} (2\kappa' \tau + \kappa \tau') + O(d, e)^4 \right).
\end{aligned} \tag{6}$$

*This estimation is optimal among all three-point approximations of the tangent in the sense that the quadratic term in the normal component cannot be different from the one that shows up here. Also, this is the only linear combination of  $\mathbf{d}$  and  $\mathbf{e}$  that yields a second order approximation.*

*Proof.* The equation can directly be derived from the Taylor expansions in Appendix A. If there were curves with other quadratic terms we could gain a tangent estimation and in turn an estimation of the normal for planar curves of the same accuracy, but this is not possible, see [ABS02].

The last statement of the proposition can easily be derived using the Taylor expansions of  $\mathbf{d}$  and  $\mathbf{e}$  from Appendix A.  $\square$

Note that in the planar case, knowledge of tangent and normal is equivalent. Therefore, every tangent formula can be used to compute normals of plane curves. In 3D, the computation of normals is more difficult, however, because the osculating plane is unknown. It can be done after estimating the binormals which determine that plane. A more direct approach is to compute the curvature vector, for example by using finite differences.

**2.2 Proposition (curvature vector).** *The finite difference approach yields a linear approximation of the true curvature vector, and thus of the true normal vector:*

$$\begin{aligned}
\bar{\mathbf{k}} &:= \frac{2}{d+e} \left( \frac{\mathbf{e}}{e} - \frac{\mathbf{d}}{d} \right) \\
&= \mathbf{t} \left( \frac{d-e}{4} \kappa^2 - \frac{d^2-de+e^2}{6} \kappa \kappa' + O(d, e)^3 \right) \\
&\quad + \mathbf{n} \left( \kappa - \frac{d-e}{3} \kappa' + \frac{d^2-de+e^2}{12} (\kappa'' - \kappa \tau^2) + O(d, e)^3 \right) \\
&\quad + \mathbf{b} \left( \frac{d-e}{3} \kappa \tau - \frac{d^2-de+e^2}{12} (2\kappa' \tau + \kappa \tau') + O(d, e)^3 \right).
\end{aligned} \tag{7}$$

Furthermore, this is the only linear combination of  $\mathbf{d}$  and  $\mathbf{e}$ , that yields a linear approximation of the real normal vector.

*Proof.* Again all claims can directly be proven from the Taylor expansions given in Appendix A.  $\square$

From the curvature vector we gain the curvature as the norm. Another possibility is to estimate the curvature by *angle approximation*. That approach is based on the definition of curvature as the rate of angular change of the tangent vector along the curve.

**2.3 Proposition (curvature).** *Let  $\varphi$  be the angle between  $\mathbf{d}$  and  $\mathbf{e}$ , see Figure 1. Curvature, estimated using the discrete curvature vector (7) or angle approximation, respectively, is given by*

$$\begin{aligned}
\bar{\kappa} &:= \|\bar{\mathbf{k}}\| \\
&= \kappa + \frac{e-d}{3} \kappa' + \frac{d^2-de+e^2}{12} \kappa'' - \frac{d^2+de+e^2}{36} \kappa \tau^2 + \frac{d^2-2de+e^2}{32} \kappa^3 + O(d, e)^3 \\
\hat{\kappa} &:= \frac{2\varphi}{d+e} = \kappa + \frac{e-d}{3} \kappa' + \frac{d^2-de+e^2}{12} (\kappa'' + \frac{\kappa^3}{2}) - \frac{d^2+de+e^2}{36} \kappa \tau^2 + O(d, e)^3
\end{aligned}$$

These estimations are optimal among all three-point approximations in the sense that the linear terms cannot be different from the ones that show up here.

*Proof.* Again the equations can be derived from Appendix A and optimality can be reduced to the planar case [ABS02].  $\square$

Yet another way to estimate the curvature is as the inverse of the radius of the circle passing through  $P_{-1}$ ,  $P_0$  and  $P_1$ . This has been done in [Bou00] and yields

$$\tilde{\kappa} = \kappa + \frac{e-d}{3} \kappa' + \frac{d^2-de+e^2}{12} \kappa'' - \frac{d^2+de+e^2}{36} \kappa \tau^2 + O(d, e)^3.$$

Since  $\sin \varphi$  equals  $\varphi$  up to quadratic error we can compute an approximation for  $\kappa$  as

$$\frac{2\|\mathbf{d} \times \mathbf{e}\|}{de(d+e)} \approx \hat{\kappa}$$

without significant loss of accuracy.

Also note that for  $d = e$  the expansion of the angle approximation becomes

$$\hat{\kappa} = \kappa + \frac{e^2}{12}(\kappa'' + \frac{\kappa^3}{2} - \kappa\tau^2) + O(e^4),$$

see Appendix A, and here the quadratic term vanishes for a special class of curves called elastica, characterized by minimizing the bending energy

$$\int \kappa^2 ds \longrightarrow \min$$

while fixing end points. They were first introduced by Euler [Eul44] and have applications in computer vision today [Mum94, Hor83].

**2.4 Proposition (elastica).** *The curvature estimation  $\hat{\kappa}$  converges of (at least) fourth order for elastica if all edges have equal length.*

In fact, the lower order error terms vanish for an even broader class of curves, see Appendix C for a derivation.

Binormals at  $P_i$  can be estimated by the normal of the plane defined by three consecutive points,  $P_{i-1}$ ,  $P_i$ , and  $P_{i+1}$ , for example  $\mathbf{b}_0 = \frac{\mathbf{d} \times \mathbf{e}}{\|\mathbf{d} \times \mathbf{e}\|}$ . Now we can apply the method of angle approximation to these binormals to compute the torsion  $\hat{\tau}_e$  (located at the edge  $\mathbf{e}$ ) from the angle  $\eta_e$  between  $\mathbf{b}_0$  and  $\mathbf{b}_1$ ,  $\|\mathbf{b}_1 \times \mathbf{b}_0\| = \sin \eta_e$ . But instead of taking the norm, which is computationally rather expensive, and even worse, always yields positive values (as do most other methods as well), whereas torsion is a signed property, we use the fact from the Frenet equations that  $\frac{d\mathbf{b}}{ds} = \tau \mathbf{n}$ . Therefore,  $\mathbf{b}_1 \times \mathbf{b}_0$  should be approximately aligned with  $\mathbf{t}$  and we define  $\hat{\eta}_e := \langle \mathbf{b}_1 \times \mathbf{b}_0, \tilde{\mathbf{t}} \rangle$  where  $\tilde{\mathbf{t}}$  denotes the tangent approximation from equation (6). In fact  $\hat{\eta}_e = \eta_e + O(d, e, f)^3$  (because  $\eta$  depends linearly on  $d$ ,  $e$  and  $f$ , and  $\sin \eta$  approximates  $\eta$  up to second order). We define  $\hat{\eta}_d$  analogously from  $\mathbf{b}_{-1}$  and  $\mathbf{b}_0$  and get (see Appendix A for the Taylor expansion of  $\hat{\eta}_e$ )

**2.5 Proposition (torsion).** *Using four of the five points  $P_{-2}$ ,  $P_{-1}$ ,  $P_0$ ,  $P_1$  and  $P_2$  we have the following approximations for torsion:*

$$\begin{aligned} \hat{\tau}_d &:= \frac{3\hat{\eta}_d}{c+d+e} = \tau - \frac{c-e}{6} \frac{\kappa'}{\kappa} \tau - \frac{c+2d-e}{4} \tau' + O(c, d, e)^2, \\ \hat{\tau}_e &:= \frac{3\hat{\eta}_e}{d+e+f} = \tau + \frac{f-d}{6} \frac{\kappa'}{\kappa} \tau - \frac{d-2e-f}{4} \tau' + O(d, e, f)^2. \end{aligned}$$

It is interesting to compare the above estimation with the results from [Bou00]:  
Let  $g$  be the distance  $\|\overrightarrow{P_0P_2}\|$ . Then

$$\tilde{\tau}_1 = \tau + \frac{d - e + 3g}{6} \frac{\kappa'}{\kappa} \tau + \frac{e - d + g}{4} \tau' + O(d, e, f)^2$$

and

$$\tilde{\tau}_2 = \tau + \frac{d + e + g}{6} \frac{\kappa'}{\kappa} \tau + \frac{e - d + g}{4} \tau' + O(d, e, f)^2.$$

Our approximation is more symmetric in the sense that the first linear error term vanishes if all edge lengths are equal. By estimating torsion using the angle between  $\mathbf{b}_{-1}$  and  $\mathbf{b}_1$ , we can get an expression completely without linear terms if  $d = e$  and  $c = f$ :

$$\begin{aligned} \tilde{\tau} := \frac{3\tilde{\eta}}{c + 2(d + e) + f} &= \tau - \frac{c^2 + cd + d^2 - e^2 - ef - f^2}{6(c + 2(d + e) + f)} \frac{\kappa'}{\kappa} \tau \\ &\quad - \frac{c^2 + 3cd + 3d^2 - 3e^2 - 3ef - f^2}{4(c + 2(d + e) + f)} \tau' + O(c, d, e, f)^2. \end{aligned}$$

Another possibility to get such a symmetric expression is to take the (unique) weighted average of  $\hat{\tau}_d$  and  $\hat{\tau}_e$  such that the term involving  $\tau'$  vanishes completely and the term involving  $\frac{\kappa'}{\kappa} \tau$  vanishes for  $d = e$  and  $c = f$ :

$$\begin{aligned} \hat{\tau} &:= \frac{1}{c + d + e + f} ((f + 2e - d)\tau_d + (c + 2d - e)\tau_e) \\ &= \tau - \frac{ce - e^2 + d^2 - df}{3(c + d + e + f)} \frac{\kappa'}{\kappa} \tau + O(c, d, e, f)^2. \end{aligned}$$

It can be further improved by estimating  $\frac{\kappa'}{\kappa} \tau$  and eliminating the corresponding error term. In that way, we can get a five-point approximation of the torsion at  $P_0$  that converges quadratically for arbitrary edge lengths.

For this purpose, we approximate curvatures at  $P_{-1}$  and  $P_1$  from the angles  $\varphi_{-1}$  between  $\mathbf{c}$  and  $\mathbf{d}$ , and  $\varphi_1$  between  $\mathbf{e}$  and  $\mathbf{f}$ :

$$\kappa_{-1} := \frac{2\varphi_{-1}}{c + d} = \kappa - \frac{c + 2d}{3} \kappa' + O(c, d)^2$$

and

$$\kappa_1 := \frac{2\varphi_1}{e + f} = \kappa + \frac{f + 2e}{3} \kappa' + O(e, f)^2.$$

From this, we get five-point estimates for curvature

$$\kappa_5 := \frac{1}{c + 2(d + e) + f}((2e + f)\kappa_{-1} + (c + 2d)\kappa_1) = \kappa + O(c, d, e, f)^2,$$

for its derivative (as suggested in [Bou00])

$$\kappa'_5 := \frac{3}{c + 2(d + e) + f}(\kappa_1 - \kappa_{-1}) = \kappa' + O(c, d, e, f),$$

and for torsion

$$\tau_5 := \hat{\tau} + \frac{ce - df + d^2 - e^2}{3(c + d + e + f)} \frac{\kappa'_5}{\kappa_5} \hat{\tau} = \tau + O(c, d, e, f)^2.$$

The last equation shows that it is possible to obtain a second order approximation for torsion using only five points.

## 3 Mesh normals

### 3.1 Averaging of face normals

Our approach to assess discrete approximation schemes for normals is to compare the normal of an arbitrary analytical surface with the estimated normal at the same point. For this purpose we determine an appropriate coordinate system such that the estimated normal can be expressed only in terms of directional curvatures, geodesic torsions and their derivatives at that point. These could, in turn, be expressed in terms of the principal curvatures and their derivatives, but this is of no relevance for the asymptotic analysis and we do not pursue it. An appropriate coordinate system will probably include the normal  $\mathbf{n}$  itself and two further orthonormal vectors, let's call them  $\mathbf{t}$  and  $\mathbf{v}$ . Then a good approximation for the normal would look like this:

$$\mathbf{n}_{\text{estimated}} = (1 + \epsilon)\mathbf{n} + \epsilon'\mathbf{t} + \epsilon''\mathbf{v}$$

where the  $\epsilon$ s are supposed to be small and should tend to zero if a denser mesh is regarded. If this is not the case, we might be able to give a good approximation for the  $\epsilon$ s to improve the approximation of  $\mathbf{n}$ .

Consider a dense mesh  $\mathcal{M}$  interpolating a smooth surface  $\mathcal{S}$  and a mesh vertex  $P$ . Let  $Q_1, Q_2, \dots, Q_n$  be the immediate neighbors of  $P$ , ordered counter-clockwise with respect to the chosen normal, see Figure 2. For each  $Q_i$ , consider the geodesic curve  $\mathbf{g}_i(s)$ , parameterized by arc length  $s$ , connecting  $P$  with  $Q_i$ ,

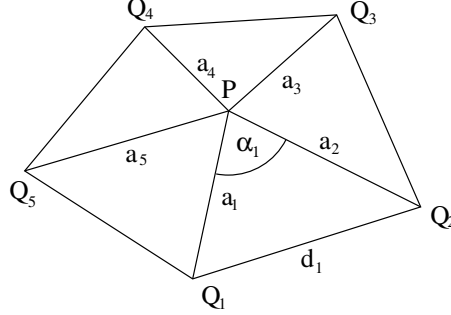


Figure 2: One-ring of a vertex.

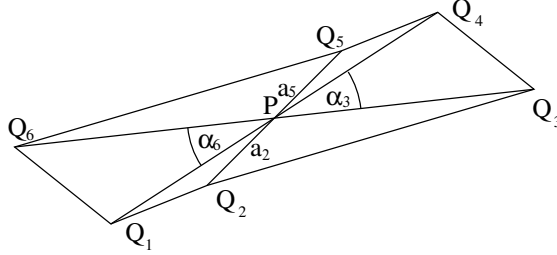


Figure 3: Example of a regular vertex.

$\mathbf{g}_i(0) = P$ . For each geodesic  $\mathbf{g}_i(s)$  consider its Darboux frame  $\{\mathbf{t}_i, \mathbf{v}_i, \mathbf{n}\}$  for  $s = 0$ :  $\mathbf{n}$  is the unit surface normal at  $\mathbf{g}_i(0)$ ,  $\mathbf{t}_i = \frac{d\mathbf{g}_i(s)}{ds}|_{s=0}$  is the unit tangent vector, and  $\mathbf{v}_i = \mathbf{n} \times \mathbf{t}_i$ .

Let  $\mathbf{a}_i := \overrightarrow{PQ_i}$  and let  $\alpha_i$  be the angle between  $\mathbf{a}_i$  and  $\mathbf{a}_{i+1}$  (indices taken modulo  $n$ ). Now we can compute the normal of an incident triangle at  $P$  as

$$\begin{aligned} \frac{\mathbf{a}_i \times \mathbf{a}_{i+1}}{\|\mathbf{a}_i \times \mathbf{a}_{i+1}\|} &= \mathbf{n} \left( 1 + O(a_i, a_{i+1})^2 \right) \\ &\quad - \mathbf{v}_i \left( \frac{a_{i+1}}{2 \sin \alpha_i} \kappa_{i+1} + O(a_i, a_{i+1})^2 \right) + \mathbf{v}_{i+1} \left( \frac{a_i}{2 \sin \alpha_i} \kappa_i + O(a_i, a_{i+1})^2 \right) \\ &\quad + \mathbf{t}_i \left( O(a_i, a_{i+1})^2 \right) + \mathbf{t}_{i+1} \left( O(a_i, a_{i+1})^2 \right), \end{aligned}$$

where  $\kappa_i$  denotes the normal curvature in direction  $\mathbf{t}_i$ , see Appendix B. This shows that the triangle normal, and therefore every normal computed as a weighted average of the triangle normals in the one-ring of  $P$ , converges linearly to the real normal, as has already been shown by Meek and Walton [MW00].

But we can prove even quadratic convergence for regular vertices<sup>1</sup>. These

<sup>1</sup>For area weighted normals, this has already been proved in [MW00] in the case  $n = 4$ , all

shall be vertices of even valence, where opposing edges have the same length, and opposing angles are equal, see Figure 3. More rigorously, we define

**3.1 Definition (regular vertex).** Let  $P$  be a mesh vertex of valence  $n = 2m$  with incident edges  $\mathbf{a}_i$  of length  $a_i$ . Let  $\alpha_i$  be the angle between  $\mathbf{a}_i$  and  $\mathbf{a}_{i+1}$ . Then  $P$  is called *regular* iff

$$a_i = a_{i+m} \quad \text{and} \quad \alpha_i = \alpha_{i+m}$$

for all  $i = 1 \dots m$ .

For regular vertices we can conclude

$$\mathbf{v}_{i+m} = -\mathbf{v}_i + O(a_j)^2 \quad \text{and} \quad \kappa_{i+m} = \kappa_i + O(a_j)^2,$$

see Appendix B. Therefore, the linear terms cancel out when summing up all facet normals of the faces incident at  $P$ . Summarizing, we can state

**3.2 Theorem (mesh normals).** Let  $P$  be a mesh vertex with incident edges  $\mathbf{a}_i$  of length  $a_i$  connecting  $P$  with  $Q_i$ . Let  $\alpha_i$  be the angle between  $\mathbf{a}_i$  and  $\mathbf{a}_{i+1}$  and let  $\mathbf{n}_i := \frac{\mathbf{a}_i \times \mathbf{a}_{i+1}}{\|\mathbf{a}_i \times \mathbf{a}_{i+1}\|}$ . Let  $w_i$  be weights depending only on edge lengths and enclosed angles. Then

$$\frac{\sum_{i=1}^n w_i \mathbf{n}_i}{\|\sum_{i=1}^n w_i \mathbf{n}_i\|}$$

converges linearly to the real normal as edge lengths  $a_i$  tend to zero if all  $\alpha_i$  are bounded within  $(0, \pi)$  (meaning that there is a  $\delta > 0$  such that always  $\delta < \alpha_i < \pi - \delta$  for all  $\alpha_i$ ).

If  $P$  is a regular vertex the convergence is even quadratic.

*Proof.* We have already shown the linear convergence. For regular vertices we get by the above arguments

$$\begin{aligned} & \sum_i w_i \frac{\mathbf{a}_i \times \mathbf{a}_{i+1}}{\|\mathbf{a}_i \times \mathbf{a}_{i+1}\|} \\ &= \sum_i \mathbf{n} w_i (1 + O(a_i, a_{i+1})^2) + \sum_i \mathbf{v}_i (O(a_i, a_{i+1})^2) + \sum_i \mathbf{t}_i (O(a_i, a_{i+1})^2). \quad \square \end{aligned}$$

We have also computed the angular error of the facet normal  $\mathbf{n}_i$ , for details see Appendix B. It seems sensible to us to interpret the inverse of that approximated error as confidence values for the respective normals. Using these values as weights for the faces incident at  $P$  yields

$$\tilde{\mathbf{n}} := \frac{\sum_i \frac{\sin \alpha_i}{d_i} \mathbf{n}_i}{\|\sum_i \frac{\sin \alpha_i}{d_i} \mathbf{n}_i\|}$$

where  $d_i$  is the length of the triangle edge opposing  $P$ , see Figure 2.

---

edges and angles equal.

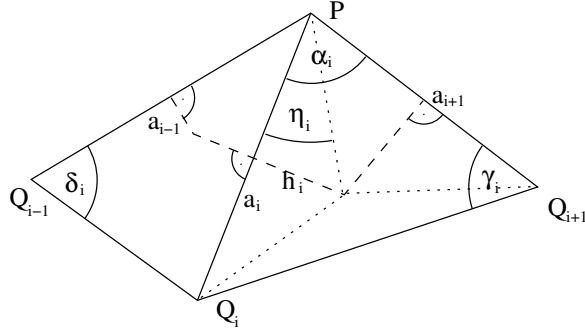


Figure 4: Cotangent weights and Voronoi area.

### 3.2 Averaging of edges

Now we turn our attention to the mean curvature vector  $\mathbf{k}$  at  $P$ . We use an approximation similar to the one in the paper of Meyer et al. [MDSB02]. That is, we approximate the integral over the mean curvature vector in a certain environment of  $P$  and divide by the corresponding area  $A$ . Using the notation of Figure 4, let  $w_i := \cot \gamma_i + \cot \delta_i$  and let  $A := \frac{1}{8} \sum_i w_i a_i^2$  be the Voronoi area of the one-ring of  $P$ .  $A$  can be computed in terms of  $\gamma_i$  and  $\delta_i$  because  $\eta_i = \frac{\pi}{2} - \gamma_i$ . We define

$$\mathbf{k} := \frac{1}{4A} \sum_i w_i \mathbf{a}_i = 2 \frac{\sum_i w_i \mathbf{a}_i}{\sum_i w_i a_i^2}.$$

This formula has already been suggested, up to a factor of two, in [DMSB99] as a “normalized version of the curvature operator”. We argue that it is not merely a normalized version but the correct (discrete) mean curvature vector.

In contrast to [MDSB02], where a “mixed region” for  $A$  has been used to ensure that it lies completely within the one-ring of  $P$ , we always use the Voronoi region. The reason for this becomes clear in Theorem 4.1 where we show why these regions determine the “right” area whereas the mixed regions seem somewhat artificial to us. Note that our approach is still compatible with the derivation given in [MDSB02]: the boundary of our “Voronoi region” (dashed lines in Figures 4 and 5) passes through the midpoints of the edges  $\mathbf{a}_i$ , and all “Voronoi regions” of the complete mesh together guarantee a perfect tessellation without overlapping if we allow “negative areas”: even though the Voronoi cell at the obtuse angle exceeds the area of the triangle in Figure 5 a), this is compensated by the “Voronoi cells” at the acute angles that count the same area negative (Figure 5 b)).

**3.3 Theorem (normal approximation).** *Let  $P$  be a mesh vertex and  $\mathbf{k}$  be the approximated mean curvature vector at  $P$  as above. Then  $\mathbf{k}$  converges linearly against the real normal vector of the same length.*

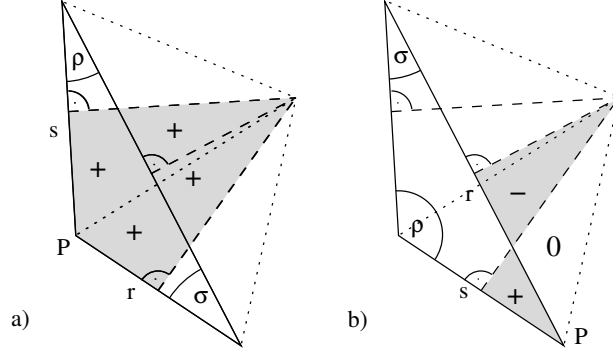


Figure 5: Voronoi areas, as computed by the formula  $\frac{1}{8}(r^2 \cot \rho + s^2 \cot \sigma)$ , give an exact tiling of the triangle. Shown are the “Voronoi areas” of an a) obtuse angle, b) acute angle.

*If  $P$  is regular, the convergence is even quadratic.*

*Proof.* Using the Taylor expansion of  $\frac{a_i}{a_i}$  in Appendix B, we get

$$\begin{aligned}
4A \cdot \mathbf{k} &:= \sum_i w_i \mathbf{a}_i = \sum_i \mathbf{t}_i \left( w_i a_i - \frac{w_i a_i^3}{8} \kappa_i^2 + O(a_i^4) \right) \\
&\quad + \sum_i \mathbf{v}_i \left( -\frac{w_i a_i^3}{6} \kappa_i \tau_i + O(a_i^4) \right) \\
&\quad + \mathbf{n} \sum_i \left( w_i \frac{a_i^2}{2} \kappa_i + w_i \frac{a_i^3}{6} \kappa_i' + O(a_i^4) \right).
\end{aligned}$$

Therefore, we have to show that  $\sum_i w_i a_i \mathbf{t}_i = O(a_i)^3$ . Then we obtain

$$\begin{aligned}
4A \cdot \mathbf{k} &= \sum_i \mathbf{t}_i \left( -\frac{w_i a_i^3}{8} \kappa_i^2 + O(a_{i-1}, a_i, a_{i+1})^3 \right) \\
&\quad + \sum_i \mathbf{v}_i \left( -\frac{w_i a_i^3}{6} \kappa_i \tau_i + O(a_i^4) \right) \\
&\quad + \mathbf{n} \sum_i \left( w_i \frac{a_i^2}{2} \kappa_i + w_i \frac{a_i^3}{6} \kappa_i' + O(a_i^4) \right).
\end{aligned} \tag{8}$$

Since all the angles and consequently the weights  $w_i$  converge quadratically to respective values in the tangent plane, we may assume that the one-ring of  $P$  is already planar and  $\mathbf{a}_i = a_i \mathbf{t}_i$ . Let  $\mathbf{h}_i$  be the part of the Voronoi edge separating  $P$  and  $Q_i$  that connects  $\overrightarrow{PQ_i}$  to the circumcenter of the triangle  $\triangle PQ_i Q_{i+1}$ , see Figure 4.

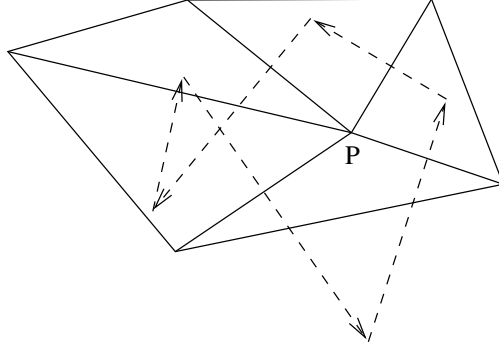


Figure 6: Complete Voronoi area.

From  $\eta_i = \frac{\pi}{2} - \gamma_i$  we conclude  $\mathbf{h}_i = (\frac{1}{2} \cot \gamma_i \mathbf{a}_i)^\perp$ , where  $()^\perp$  is the  $\frac{\pi}{2}$  counter-clockwise rotation. Now it suffices to show that the sum of the Voronoi edges  $\sum_i w_i \mathbf{a}_i^\perp$  is zero, but this is clear, compare Figure 6. Note that this may not be a Voronoi region in the usual sense, but it retains the important property that it forms a closed curve.

For regular vertices, we know  $a_i = a_{i+m}$  and  $\alpha_i = \alpha_{i+m}$ , and therefore,  $w_i = w_{i+m}$ ,  $\kappa_i \approx \kappa_{i+m}$ , and  $\tau_i \approx \tau_{i+m}$ , see Appendix B. This means that the third order terms, which are explicitly given in the tangential components of equation (8), vanish, and a careful examination shows that also the  $O(a_{i-1}, a_i, a_{i+1})^3$  terms, stemming from the computations above, cancel.  $\square$

## 4 Curvature Tensor

In this section, we will analyze the asymptotic behavior of the (modified) mean curvature vector as defined in [MDSB02]. We will show its limitations and suggest a novel weighting scheme for better approximation of the mean curvature. Furthermore, we will show how this approach can be extended to gain accurate estimates of Gaussian curvature and the curvature directions.

### 4.1 Mean curvature vector

**4.1 Theorem (mean curvature approximation I).** *Let*

$$\mathbf{k} := 2 \frac{\sum_i (\cot \gamma_i + \cot \delta_i) \mathbf{a}_i}{\sum_i (\cot \gamma_i + \cot \delta_i) a_i^2}$$

*be the mean curvature vector at P defined in Section 3.2. Let all edge lengths  $a_i$  be equal and let all angles  $\alpha_i$  be equal. Then  $\|\mathbf{k}\|$  converges linearly towards the*

real mean curvature.

If the edge lengths  $a_i$  and angles  $\alpha_i$  are varying then  $\|\mathbf{k}\|$  will in general not converge towards the correct mean curvature.

*Proof.* Under the assumption that all the  $a_i$  and  $\alpha_i$  are equal, the angles  $\gamma_i$  and  $\delta_i$  and therefore the weights  $w_i$  have to be equal for all  $i$  as well. Using formula (8) we obtain  $\|\mathbf{k}\| = \sum_i \frac{w_i a_i^2}{\sum_i w_i a_i^2} \kappa_i + O(a_i) = \frac{1}{n} \sum_i \kappa_i + O(a_i)$ . The last term is known to be exactly the mean curvature, since the angles  $\alpha_i$  are equal and the directional curvatures  $\kappa_i$  are evenly distributed, compare the proof of Theorem 4.2.

This argumentation doesn't hold in the general case of course. For example, it can be that all directional curvatures  $\kappa_i$  and therefore the result of the cotangent formula are smaller than the mean curvature.  $\square$

Therefore, the cotangent weights are not appropriate to get the correct mean curvature with differing edge lengths and angles, even though they are very well suited to obtain the correct normal. Now note that the mean curvature is always given by the normal component of the mean curvature vector  $\mathbf{k}$ . That means, that we can use better weights if we can ensure by other means that the tangential components of  $\mathbf{k}$  vanish. This is the case for regular vertices. Alternatively, if we already know the exact normal (at least up to quadratic error) we can use it to extract the normal component of  $\mathbf{k}$ . This motivates

**4.2 Theorem (mean curvature approximation II).** *If  $P$  is regular, then the normal component of*

$$\bar{\mathbf{k}} := 2 \frac{\sum_i (\tan \alpha_{i-1} + \tan \alpha_i) \frac{\mathbf{a}_i}{a_i^2}}{\sum_i (\tan \alpha_{i-1} + \tan \alpha_i)}$$

*converges linearly towards the mean curvature at  $P$ .*

*Proof.* Let  $\bar{w}_i := \tan \alpha_{i-1} + \tan \alpha_i$ . If we insert the asymptotic expansion into the above formulae, we get  $\langle \bar{\mathbf{k}}, \mathbf{n} \rangle = \frac{1}{\sum_i \bar{w}_i} \sum_i \bar{w}_i \kappa_i + O(a_i)$ . (This reduces to  $\frac{1}{n} \sum_i \kappa_i + O(a_i)$  if all angles  $\alpha_i$  are equal.) Let  $\phi_i$  be the angle between the principal direction of maximal curvature and  $\mathbf{t}_i$ . Euler's formula yields

$$\begin{aligned} \frac{1}{\sum_i \bar{w}_i} \sum_i \bar{w}_i \kappa_i &= \frac{\kappa_{\max}}{\sum_i \bar{w}_i} \sum_i \bar{w}_i \cos^2 \phi_i + \frac{\kappa_{\min}}{\sum_i \bar{w}_i} \sum_i \bar{w}_i \sin^2 \phi_i \\ &= \frac{\kappa_{\max}}{\sum_i \bar{w}_i} \sum_i \bar{w}_i \frac{1 + \cos 2\phi_i}{2} + \frac{\kappa_{\min}}{\sum_i \bar{w}_i} \sum_i \bar{w}_i \frac{1 - \cos 2\phi_i}{2} \\ &= \frac{\kappa_{\max} + \kappa_{\min}}{2} + \frac{\kappa_{\max} - \kappa_{\min}}{2 \sum_i \bar{w}_i} \operatorname{Re} \left( \sum_j \bar{w}_j e^{2i\phi_j} \right). \end{aligned}$$

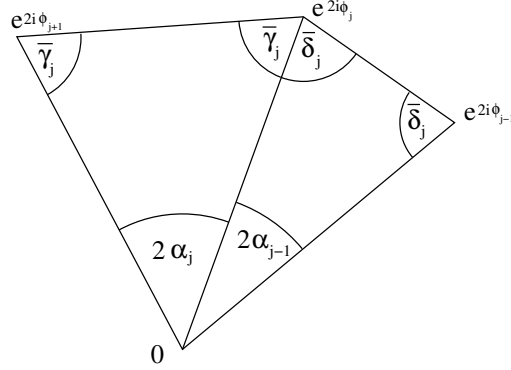


Figure 7: Weights for computation of the mean curvature.

Now it is sufficient to show that  $\sum_j \bar{w}_j e^{2i\phi_j} = 0$ . If we consider  $e^{2i\phi_j}$  as the vertices of a one-ring with the origin of the complex plane as center, then we know already, from the proof of Theorem 3.3, that the correct weights are  $\cot \bar{\gamma}_j + \cot \bar{\delta}_j$ , see Figure 7. But since all the edges  $e^{2i\phi_j}$  have the same length, we can compute  $\cot \bar{\gamma}_j + \cot \bar{\delta}_j = \cot \frac{\pi - 2\alpha_j}{2} + \cot \frac{\pi - 2\alpha_{j-1}}{2} = \bar{w}_j$ .  $\square$

The formula  $2\langle \frac{\mathbf{a}_i}{a_i^2}, \mathbf{n} \rangle$  has already been used by Taubin [Tau95a] to gain an approximation of  $\kappa_i$  and in turn also of the mean curvature. Numerous other methods exist to approximate the mean curvature, see for example [Boi95]. But at least so far we haven't been able to prove asymptotic correctness for them.

## 4.2 Quadratures for curvature integrals

Now we adopt another point of view concerning our formula to approximate mean curvature. It can be seen as the approximation of an exact quadrature of the mean curvature integral (3). This viewpoint proves to be powerful and extensible to the computation of Gaussian curvature and the curvature tensor.

Given a point  $P$  on a smooth surface  $S$ , consider its tangent plane that is spanned by two unit vectors in the principal directions  $\mathbf{t}_{\max}$  and  $\mathbf{t}_{\min}$ , see Figure 8 on the left hand side. The curvatures in these directions are given by  $\kappa_{\max}$  and  $\kappa_{\min}$ , respectively. Assume now that  $\mathbf{t}_i$ ,  $i = 1..n$  are further unit tangent vectors. Let  $\phi_i$  be the angle between  $\mathbf{t}_{\max}$  and  $\mathbf{t}_i$  measured counter-clockwise and let  $\beta_i := \phi_{i+1} - \phi_i$  (indices modulo  $n$ ) be the angle between  $\mathbf{t}_{i+1}$  and  $\mathbf{t}_i$ . Let  $\kappa_i$  be the normal curvature of  $S$  at  $P$  in direction  $\mathbf{t}_i$ . More general, let  $\mathbf{t}(\phi)$  be the unit tangent vector with angle  $\phi$  to  $\mathbf{t}_{\max}$  and  $\kappa(\phi)$  the normal curvature in that direction. Now we will show how mean curvature, Gaussian curvature and the curvature tensor can be computed only from the knowledge of the  $\kappa_i$  and  $\beta_i$ . (Discrete estimations for  $\kappa_i$  and  $\beta_i$

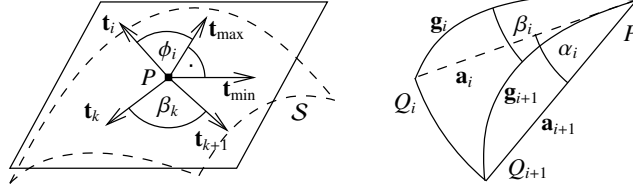


Figure 8: Angles in tangent plane and mesh.

are given in Section 4.3.)

### Mean curvature

In this paragraph, we will present a formula to compute the mean curvature  $H$ . It can be seen as a generalization of a result from mathematical folklore that states  $H = \frac{1}{n} \sum_i \kappa_i$  which, again, is a generalization of  $H = \frac{1}{2}(\kappa_{\max} + \kappa_{\min})$ . We prefer to regard it as a quadrature  $\sum_i w_i \kappa_i$  of curvature integral (3) with certain weights  $w_i$  that add up to one:

$$w_j := \frac{\tan \beta_{j-1} + \tan \beta_j}{\sum_k (\tan \beta_{k-1} + \tan \beta_k)}. \quad (9)$$

They have the property

$$\sum_i w_i \cos 2\phi_i = 0$$

as shown in the proof of Theorem 4.2, and we arrive at

**4.3 Theorem.** *Mean curvature is given by the weighted sum of normal curvatures with the weights defined in (9):*

$$H = \sum_i w_i \kappa_i.$$

### Gaussian curvature

To obtain the Gaussian curvature  $K$  we have to compute the integral  $G := \frac{1}{2\pi} \cdot \int_0^{2\pi} \kappa(\phi)^2 d\phi$  from Equation (4). Again with Euler's formula (1) we obtain an approximation of that integral:

$$\begin{aligned} \tilde{G} := \sum_i \tilde{w}_i \kappa_i^2 &= \frac{3}{2} H^2 - \frac{1}{2} K + \\ &\sum_i \tilde{w}_i \left( \frac{4 \cos 2\phi_i + \cos 4\phi_i}{8} \kappa_{\max}^2 - \frac{4 \cos 2\phi_i - \cos 4\phi_i}{8} \kappa_{\min}^2 - \frac{\cos 4\phi_i}{4} K \right). \end{aligned}$$

Here we exploit  $\sum_j \tilde{w}_j e^{4i\phi_j} = 0$  for

$$\tilde{w}_j := \frac{\tan 2\beta_{j-1} + \tan 2\beta_j}{\sum_k (\tan 2\beta_{k-1} + \tan 2\beta_k)} \quad (10)$$

and therefore

$$\sum_i \tilde{w}_i \sin 4\phi_i = \sum_i \tilde{w}_i \cos 4\phi_i = 0. \quad (11)$$

With the notation  $\Sigma_{\cos} := \frac{1}{2} \sum_i \tilde{w}_i \cos 2\phi_i$  we get

$$\tilde{G} = \frac{3}{2}H^2 - \frac{1}{2}K + 2H(\kappa_{\max} - \kappa_{\min})\Sigma_{\cos}.$$

Using the same weights for the estimation of  $H$  we obtain

$$\tilde{H} := \sum_i \tilde{w}_i \kappa_i = H + (\kappa_{\max} - \kappa_{\min})\Sigma_{\cos}.$$

Therefore, we can compute the exact value of  $K$ :

**4.4 Theorem.** *Gaussian curvature can be computed from the mean curvature  $H$  and the corrected weighted sum of squares of normal curvatures with the weights defined in (10):*

$$K = 3H^2 - 2 \sum_i \tilde{w}_i \kappa_i^2 + 4H \left( \sum_i \tilde{w}_i \kappa_i - H \right).$$

### The Taubin tensor

Now we will show how the matrix  $\mathbf{M}$ , defined by integral (5), that was introduced by Taubin [Tau95a] to compute the curvature tensor, can be evaluated exactly. Afterwards, we will give an alternative method to compute the principal curvatures and directions.

Let  $\mathbf{T} := (\mathbf{n}, \mathbf{t}_{\max}, \mathbf{t}_{\min})$  be the orthogonal matrix with the columns given by the normal and the unit tangent vectors of the principal directions at the surface point  $P$ . In [Tau95a], it was shown that

$$\mathbf{M} = \mathbf{T} \begin{pmatrix} 0 & 0 & 0 \\ 0 & \lambda_1 & 0 \\ 0 & 0 & \lambda_2 \end{pmatrix} \mathbf{T}'$$

where  $\lambda_1$  and  $\lambda_2$  are the eigenvalues of  $\mathbf{M}$  that are related to the principal curvatures in the following way:

$$\kappa_{\max} = 3\lambda_1 - \lambda_2, \quad \kappa_{\min} = 3\lambda_2 - \lambda_1.$$

To compute a discrete approximation of integral (5) we use the equalities (11) for weights (10) together with Euler's formula (1) and obtain:

$$\tilde{\mathbf{M}} := \sum_i \tilde{w}_i \kappa_i \mathbf{t}_i \mathbf{t}_i^t = \mathbf{T} \begin{pmatrix} 0 & 0 & 0 \\ 0 & \lambda_1 + \kappa_{\max} \Sigma_{\cos} & H \Sigma_{\sin} \\ 0 & H \Sigma_{\sin} & \lambda_2 - \kappa_{\min} \Sigma_{\cos} \end{pmatrix} \mathbf{T}^t$$

with  $\Sigma_{\cos} := \frac{1}{2} \sum_i \tilde{w}_i \cos 2\phi_i$  and  $\Sigma_{\sin} := \frac{1}{2} \sum_i \tilde{w}_i \sin 2\phi_i$ . Again, we want to compute the error terms and subtract them afterwards as we did when computing the Gaussian curvature. However, the task is trickier this time since the error terms are given in a coordinate system yet unknown.

But let us define the error matrix

$$\tilde{\mathbf{E}} := \sum_i \tilde{w}_i \mathbf{t}_i \mathbf{t}_i^t = \mathbf{T} \begin{pmatrix} 0 & 0 & 0 \\ 0 & \frac{1}{2} + \Sigma_{\cos} & \Sigma_{\sin} \\ 0 & \Sigma_{\sin} & \frac{1}{2} - \Sigma_{\cos} \end{pmatrix} \mathbf{T}^t.$$

After restriction of the matrices to the tangent plane by a Householder transformation  $\mathbf{Q}$  as done in [Tau95a], we can eliminate most of the error terms and control the remaining ones by computing:

$$\begin{aligned} \mathbf{Q} \tilde{\mathbf{M}} \mathbf{Q}^t - H(\mathbf{Q} \tilde{\mathbf{E}} \mathbf{Q}^t - \frac{1}{2} \begin{pmatrix} 0 & 0 & 0 \\ 0 & 1 & 0 \\ 0 & 0 & 1 \end{pmatrix}) \\ = \mathbf{Q} \mathbf{T} \begin{pmatrix} 0 & 0 & 0 \\ 0 & \lambda_1 + \frac{\kappa_{\max} - \kappa_{\min}}{2} \Sigma_{\cos} & 0 \\ 0 & 0 & \lambda_2 + \frac{\kappa_{\max} - \kappa_{\min}}{2} \Sigma_{\cos} \end{pmatrix} (\mathbf{Q} \mathbf{T})^t. \end{aligned} \quad (12)$$

Now all the desired information can be extracted:

**4.5 Theorem.** *The matrix defined in equation (12) has the surface normal and the principal directions as eigenvectors. Its eigenvalues  $\mu_1$  and  $\mu_2$  corresponding to the latter two eigenvectors are related to the principal curvatures by*

$$\kappa_{\max} = 3\mu_1 - \mu_2 - (\tilde{H} - H), \quad \kappa_{\min} = 3\mu_2 - \mu_1 - (\tilde{H} - H).$$

### Direct computation of the curvature tensor

Once we know mean and Gaussian curvature, there is also a more direct approach to obtain principal curvatures and directions. First, we can compute the principal directions:

$$\kappa_{\max} = H + \sqrt{H^2 - K}, \quad \kappa_{\min} = H - \sqrt{H^2 - K}.$$

Now we use Euler's formula (1) in the form

$$\kappa_i = (\kappa_{\max} - \kappa_{\min}) \cos^2 \phi_i + \kappa_{\min}.$$

When solving for  $\phi_i$  we get two solutions for every  $i$  (modulo  $\pi$ ). Since the correct solutions coincide for all  $i$ , they can be easily determined.

### 4.3 Practical curvature tensor estimation

In this section we will discuss how the quadratures from Section 4.2 lead to a working algorithm.

#### Normal curvatures and geodesic angles

Let  $P$  be a vertex of the mesh  $\mathcal{M}$  with its one-ring given by vertices  $Q_i$  such that  $P$  and the  $Q_i$  interpolate the surface  $\mathcal{S}$ . Let  $\mathbf{a}_i$  be the edge connecting  $P$  and  $Q_i$ , let  $\mathbf{g}_i$  be the geodesic connecting  $P$  and  $Q_i$  in  $\mathcal{S}$ , and let  $\mathbf{t}_i$  be the unit tangent to  $\mathbf{g}_i$  at  $P$ . Given a (possibly estimated) unit normal vector  $\mathbf{n}$  at  $P$ , the normal curvature can be approximated as  $\kappa_i \approx 2 \frac{\langle \mathbf{a}_i, \mathbf{n} \rangle}{a_i^2}$ , where  $a_i := \|\mathbf{a}_i\|$ , see for example [Tau95a]. Furthermore,  $\beta_i$  can initially be approximated by the angle  $\alpha_i$  between  $\mathbf{a}_i$  and  $\mathbf{a}_{i+1}$ , see Figure 8 on the right hand side. The tangent vector  $\mathbf{t}_i$  can be estimated by the normalized projection of  $\mathbf{a}_i$  to the tangent plane  $\mathbf{a}'_i := \frac{\mathbf{a}_i - \langle \mathbf{a}_i, \mathbf{n} \rangle \mathbf{n}}{\|\mathbf{a}_i - \langle \mathbf{a}_i, \mathbf{n} \rangle \mathbf{n}\|}$ . Finally, the angle  $\alpha'_i$  between  $\mathbf{a}'_i$  and  $\mathbf{a}'_{i+1}$  gives a better approximation for  $\beta_i$  than  $\alpha_i$  does.

#### Convergence properties

Along with the above estimates for  $\kappa_i$ ,  $\beta_i$  and  $\mathbf{t}_i$ , we utilize the classical Darboux frame for  $\mathbf{g}_i$  to express the Taylor expansion of  $\mathcal{S}$  at  $P$  in order to prove the convergence of our formulae as the edge lengths tend to zero:

$$\frac{\mathbf{a}_i}{a_i} = \mathbf{t}_i \left(1 - \frac{a_i^2}{8} \kappa_i^2\right) + \mathbf{v}_i \left(-\frac{a_i^2}{6} \kappa_i \tau_i\right) + \mathbf{n} \left(\frac{a_i}{2} \kappa_i + \frac{a_i^2}{6} \kappa'_i\right) + \text{h. o. t.}$$

where  $\mathbf{v}_i := \mathbf{n} \times \mathbf{t}_i$ . It becomes clear that the above estimate for  $\kappa_i$  is a linear approximation of the true normal curvature provided that  $\mathbf{n}$  is at least a quadratic approximation of the correct normal. This is a reasonable assumption since it was proven in [MW00] that such an approximation can be obtained by fitting a quadratic patch to the one-ring of  $P$  if  $P$  has at least valence five. This linear error introduces a linear error in our approximations for mean curvature, Gaussian curvature and the curvature tensor.

From the same Taylor expansion, it can be seen that  $\frac{\mathbf{a}_i}{a_i}$  is already a linear approximation of  $\mathbf{t}_i$ . The projection to the tangent plane yields an even quadratic

approximation of  $\mathbf{t}_i$  by  $\mathbf{a}'_i$ . After computing the cross product of  $\mathbf{a}_i$  and  $\mathbf{a}_{i+1}$ , we conclude that  $\alpha_i$  is a quadratic approximation of  $\beta_i$  (compare [MD02]) and the same holds for  $\alpha'_i$ . The quadratic error for  $\beta_i$  yields a quadratic error for  $\tan\beta_i$  and for  $w_i$  and  $\widetilde{w}_i$ . Again these quadratic errors propagate through all our computations and add an additional quadratic error to the results of mean curvature, Gaussian curvature and curvature tensor.

### Implementation details

When computing the weights defined in (10), it may happen that the value of the denominator becomes zero or close to zero, for example if right angles are involved. In this case the weights can become very big and will enlarge small errors in the estimation of the normal curvatures greatly. To cope with a situation of a very small denominator for a vertex we omit some edges in the one-ring of that vertex. That means, we use only the subset of edges in the one-ring such that the denominator becomes maximal for the new weights. (Remember that we only need three edges to apply our method.) This improved our results for these cases.

## 5 Experimental results

In this section, we present at first detailed results of our quadrature method to compute the mean curvature; then we make a short comparison of our methods and existing approaches to compute the curvature tensor.

### 5.1 Mean curvature

We applied our newly proposed formulae for mean curvature approximation on several meshes with the vertices exactly interpolating smooth surfaces of constant mean curvature. For these meshes it is especially easy to compare the estimated values with the true values. We studied the following methods: cotangent weights using a mixed area as proposed by Meyer et al. [MDSB02], cotangent weights using Voronoi areas as defined in Theorem 4.1 and tangent weights as defined in Theorem 4.2. Since, for the last method, knowledge of the normal vectors is necessary, we compared the results when using the true normals which were available for our test surfaces, and using estimated normals with spherical weights [Max99] to study the case where the true normals are unknown. The meshes with the most interesting results and the corresponding histograms are depicted in Figure 9.

Our first test surface was a sphere with constant mean curvature  $-1$ . Since the estimated normals are identical with the true normals in this example, we forbore from using the true normals to simplify the histogram representation. While the

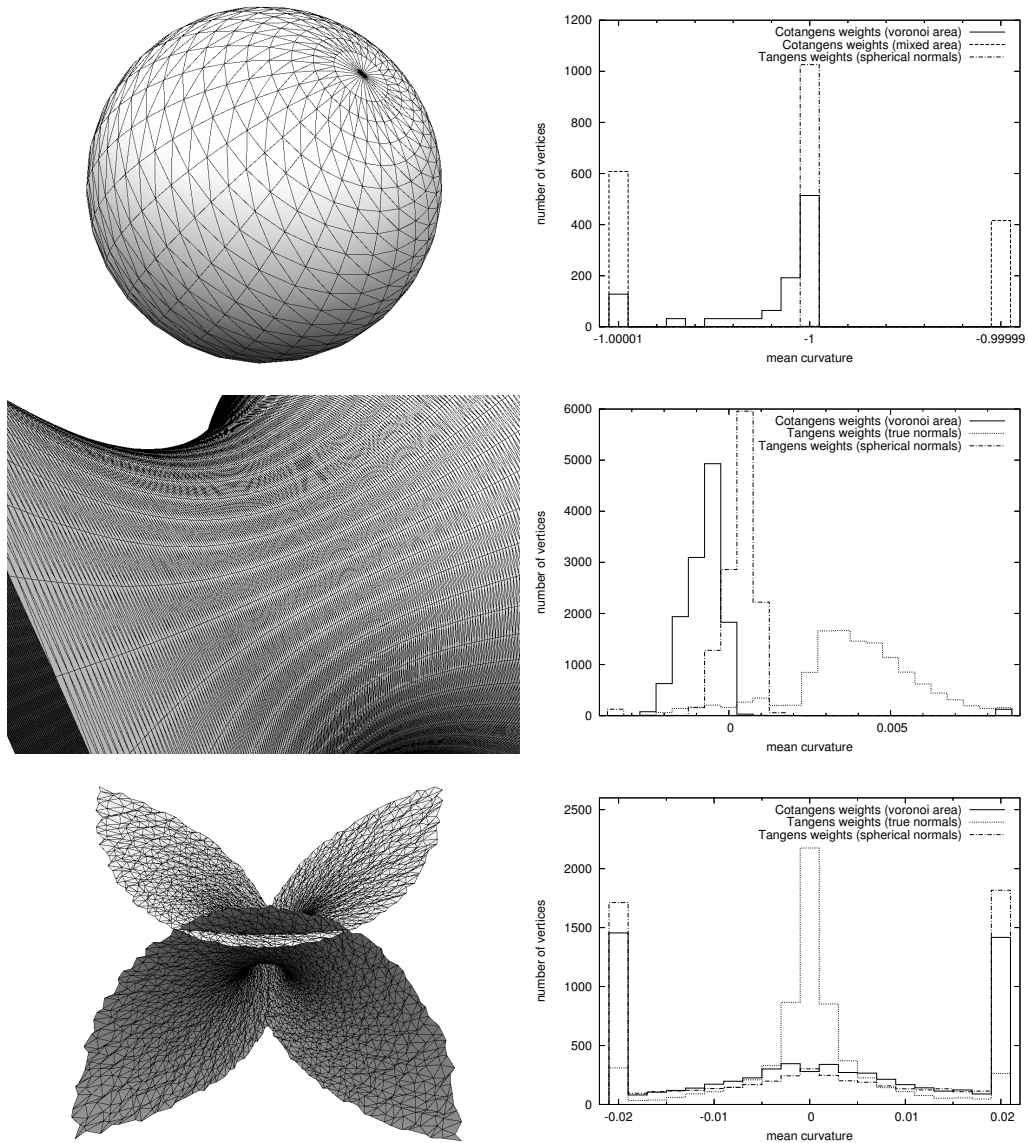


Figure 9: Some of our test shapes. From top to bottom: a polar sphere, a catenoid with strongly differing edge lengths and Enneper's surface with very irregular connectivity. On the left side is the mesh and on the right side the corresponding histogram. The leftmost and rightmost columns count not only the vertices of the specified curvature but also all vertices with lower or higher curvature, respectively.

average error using cotangent weighting with mixed areas was 0.002, the use of Voronoi areas gave much better results as can be seen in the histogram of the sphere. This clear difference is due to the fact that in the given sphere nearly every second triangle is obtuse and, in turn, nearly every vertex is affected by the different area computation. It is also remarkable that the tangent weights gave the exact value ‘ $-1$ ’ for the mean curvature within the limits of numerical precision of our implementation.

The two other test surfaces were minimal surfaces with constant mean curvature zero. For these meshes, the difference between Voronoi areas and mixed areas were less significant. Since we have already shown the superiority of using Voronoi areas by means of the first model, we haven’t included cotangent weights with mixed areas in the histograms any longer. The second surface was a catenoid with strongly differing edge lengths. With this mesh, we wanted to test our hypothesis that these differing edge lengths distort the results of the cotangent weighting. This proved to be correct as can be seen in the histogram. The majority of the curvature estimations were shifted to negative values which correspond to the direction of the longer edges. Surprisingly for us, the tangent weights with exact normals gave a shifted result as well – but to the other direction. Judging from additional tests, this could be due to the nearly rectangular angles in this mesh that pose a problem for the computation of the tangent. Still more unexpectedly, we got the best results using the merely estimated normals. Note also that the catenoid has 126 boundary vertices which can clearly be seen in the leftmost and rightmost column of the histogram for the cotangent weights and the tangent weights with spherical normals, respectively. Using the tangent weights with exact normals we obtained good results in our implementation without any special treatment of boundary vertices. Since only the normal component is used, the unbalanced situation has no effect.

Our last test surface was an irregular mesh (with 320 boundary vertices) of Enneper’s surface, a manifold that cannot completely be embedded in  $\mathbb{R}^3$  without self-intersections. Here the full power of our tangent weights approach could be observed. While the cotangent weights mean curvature estimations were scattered over a large range of values, the tangent weights method still gave good approximations of the correct value. Also, the importance of a good normal approximation could be seen here: using the estimated normals, the tangent and cotangent weights led to similar results. But note in the histogram of the cotangent method that the correct zero value seems to be avoided. This is probably an inherent problem of computing the mean curvature as the norm of a vector. A small disturbance in any direction yields a wrong value, while using only the normal components errors in tangential directions are ignored.

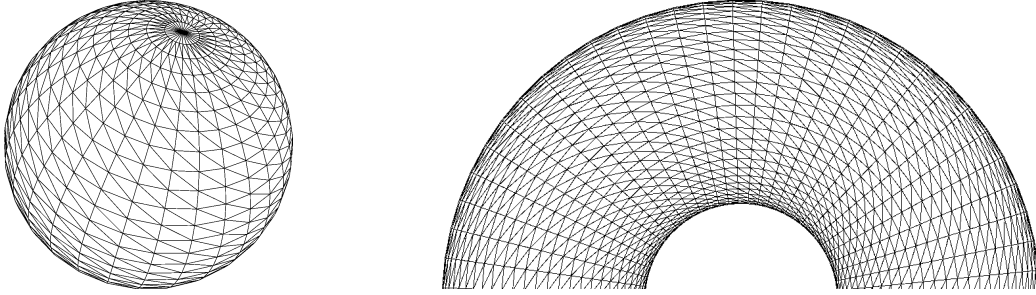


Figure 10: Meshes of a polar sphere and a regular torus.

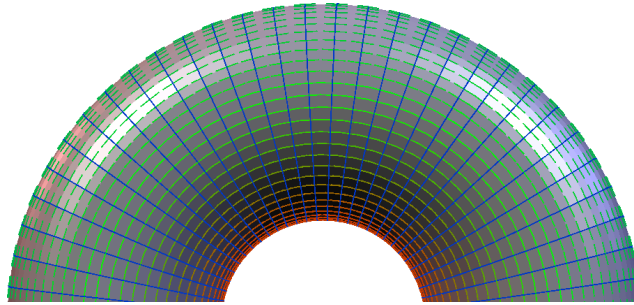


Figure 11: Principal directions (colored according to the corresponding principal curvature values decreasing from red over green to blue) of a triangulated torus.

## 5.2 Curvature tensor

We tested our algorithm on a model of a sphere with constant Gaussian curvature  $K = 1$  and on a model of a torus with Gaussian curvature varying from  $-1$  to  $\frac{1}{3}$ , both are depicted in Figure 10. The results are given in Tables 1 and 2. We measured the root-mean-square error for mean curvature  $H$ , Gaussian curvature  $K$ , the angular deviation  $\theta$  of the principal directions in radians, and the time in seconds computed on a 1.8 GHz CPU (Intel Xeon). No optimization to achieve especially short running times was done for our algorithm. We compared the following methods: (1) angle deficit in the version of Meyer et al. [MDSB02], (2) quadrature of curvature integrals as presented in this paper (principal directions via Euler’s formula); the first number gives the time for computing only the curvatures, the second number the time to compute additionally the principal directions; the results for the torus are also visualized in Figure 11, (3) the original Taubin method [Tau95a], (4) the Taubin tensor computed by exact quadrature as presented in this paper, (5) and (6) quadratic and cubic polynomial fitting as done by Goldfeather and Interrante [GI04]. All computations were done with the exact normals known.

	$H$	$K$	T (sec)
angle deficit	–	0.00465	0.02
quadrature*	$1.85 \cdot 10^{-13}$	$3.87 \cdot 10^{-13}$	0.03 / 0.06
Taubin (classic)	$3.47 \cdot 10^{-14}$	0.422	0.03
Taubin (quadrature)*	$1.81 \cdot 10^{-13}$	$3.62 \cdot 10^{-13}$	0.05
GI (quadratic)	0.00402	0.00805	0.07
GI (cubic)	0.000563	0.00113	0.16

Table 1: Error and time for a polar sphere (1026 vertices), the starred methods are developed in this paper.

	$H$	$K$	$\theta$	T (sec)
angle deficit	–	0.000901	–	0.09
quadrature*	0.00120	0.0284	0.0886	0.14/0.21
Taubin (classic)	0.0817	0.380	0.158	0.11
Taubin (quadr.)*	0.00120	0.0405	0.139	0.21
GI (quadratic)	0.00791	0.00657	0.00175	0.21
GI (cubic)	0.00456	0.00789	0.00182	0.53

Table 2: Error and time for a regular torus (3969 vertices), the starred methods are developed in this paper.

The angle deficit method is the simplest and fastest, yet it can only be used to compute the Gaussian curvature and no asymptotically correct results can be expected in general. The classical Taubin method is the fastest to compute the whole curvature tensor, but its accuracy is less than that of modern techniques. Nevertheless, if the Taubin tensor is computed using the quadrature weights as proposed in this paper, it can achieve competitive results with a small time penalty. The approach of Goldfeather and Interrante offers the best results for computing the principal directions, yet it is also the algorithm with the highest running time which limits its usefulness for very large meshes. Our approaches combine high accuracy and relatively short computation times. Furthermore, by the modular structure of method (2), running times can be further decreased if only the curvatures, but not the principal directions are needed.

## 6 Conclusion

We introduced a framework for asymptotic analysis of differential properties of discrete curves and surfaces. Using it, we have proposed formulae to compute curvature, torsion, and the Frenet frame of a space curve, and investigated their

convergence properties when edge lengths tend to zero.

We have shown that all commonly used weighting schemes for estimating vertex normals on a mesh from the normals of the incident faces converge quadratically at regular vertices. The same is true for the mean curvature vector when it is computed with cotangent weights at the edges and normalized by Voronoi areas as proposed by us.

Furthermore, we presented a new, mathematically founded method to compute mean curvature, Gaussian curvature and the curvature tensor. For the case where all edge lengths and angles are known to be equal we have even been able to prove linear convergence of the norm of the mean curvature vector, computed with cotangent weights, to the true mean curvature. In general though, we have shown that the tangent weights suggested by us are more appropriate for mean curvature computation. We have demonstrated that they yield especially superior results if used for meshes with irregular connectivity, but require knowledge of the normal vector.

In particular, we have proven theorems for exact computation of curvature integrals that lead to quite impressive results and rely only on elementary mathematics. Our experiments showed short running times and often superior results compared to existing methods. Furthermore, the method is proven to converge if normal vectors of at least quadratic accuracy are available.

In the future, we plan to extend our research to curvature and torsion of curves on surfaces. Also, we want to examine the influence of noise on normal and curvature estimations.

## Acknowledgements

The research of the authors has been supported in part by the EC-IST FP6 Network of Excellence “AIM@SHAPE”.

## References

- [ABS02] E. V. Anoshkina, A. G. Belyaev, and H.-P. Seidel. Asymptotic analysis of three-point approximations of vertex normals and curvatures. In G. Greiner, H. Niemann, T. Ertl, B. Girod, and H.-P. Seidel, editors, *Vision, Modeling, and Visualization 2002*, pages 211–216, Erlangen, Germany, November 2002.
- [ACSD<sup>+</sup>03] Pierre Alliez, David Cohen-Steiner, Olivier Devillers, Bruno Levy, and Mathieu Desbrun. Anisotropic polygonal remeshing. *ACM Transactions on Graphics. Special issue for SIGGRAPH conference*, pages 485–493, 2003.

- [BAYY99] A. G. Belyaev, E. V. Anoshkina, S. Yoshizawa, and M. Yano. Polygonal curve evolutions for planar shape modeling and analysis. *International Journal of Shape Modeling*, 5(2):195–217, 1999.
- [BCM03] V. Borrelli, F. Cazals, and J.-M. Morvan. On the angular defect of triangulations and the pointwise approximation of curvatures. *Comput. Aided Geom. Design*, 20, 2003.
- [Boi95] E. Boix. *Approximation lineaire des surfaces de  $R^3$  et applications*. PhD thesis, Ecole Polytechnique, France, 1995.
- [Bou00] M. Boutin. Numerically invariant signature curves. *International Journal of Computer Vision*, 40(3):235–248, 2000.
- [CSM03] David Cohen-Steiner and Jean-Marie Morvan. Restricted delaunay triangulations and normal cycle. In *Proceedings of the nineteenth annual symposium on Computational geometry*, pages 312–321. ACM Press, 2003.
- [dC76] Manfredo P. do Carmo. *Differential Geometry of Curves and Surfaces*. Prentice-Hall, 1976. 503 pages.
- [DFRS03] Doug DeCarlo, Adam Finkelstein, Szymon Rusinkiewicz, and Anthony Santella. Suggestive contours for conveying shape. *ACM Transactions on Graphics*, 22(3):848–855, July 2003.
- [DMSB99] M. Desbrun, M. Meyer, P. Schröder, and A. H. Barr. Implicit fairing of irregular meshes using diffusion and curvature flow. *Computer Graphics (Proceedings of SIGGRAPH 99)*, pages 317–324, 1999.
- [Eul44] Leonhard Euler. Additamentum ‘De Curvis Elasticis’. In *Methodus Inveniendi Lineas Curvas Maximi Minimive Proprietate Gaudentes*, Lausanne, 1744.
- [Eul60] Leonhard Euler. Recherches sur la courbure des surfaces. *Mem. de l’Academie des Sciences de Berlin*, 16:119–143, 1760. = [Eul76].
- [Eul76] Leonhard Euler. *Leonhardi Euleri Opera Omnia*, volume 28, pages 1–22. Teubner and O. Füssli, Leipzig-Berlin-Zürich, 1911-1976.
- [Gau27] Carl Friedrich Gauß. Disquisitiones generales circa superficies curvas. 1827. Included in [Gau65].
- [Gau65] Carl Friedrich Gauß. *General Investigations of Curved Surfaces*. Raven Press, New York, 1965.

- [GI04] Jack Goldfeather and Victoria Interrante. A novel cubic-order algorithm for approximating principal direction vectors. *ACM Trans. Graph.*, 23(1):45–63, 2004.
- [Gla90] A. S. Glassner. Computing surface normals for 3D models. In A. S. Glassner, editor, *Graphics Gems*, pages 562–566. Academic Press, 1990.
- [Gou71] H. Gouraud. Continuous shading of curved surfaces. *IEEE Transactions on Computers*, C-20(6):623–629, 1971.
- [HDW98] J. Hoschek, U. Dietz, and W. Wilke. A geometric concept of reverse engineering of shape: Approximation and feature lines. In M. Dæhlen, T. Lyche, and L. L. Schumaker, editors, *Mathematical Methods for Curves and Surfaces II*, pages 253–262. Vanderbilt Univ. Press, 1998.
- [Hor83] B. K. P. Horn. The curve of least energy. *ACM Trans. on Math. Software*, 9:441–460, 1983.
- [HS03] Eyal Hameiri and Ilan Shimshoni. Estimating the principal curvatures and the Darboux frame from real 3-d range data. *IEEE Transactions on Systems, Man, and Cybernetics, Part B*, 33(4):626–637, 2003.
- [Kat98] Victor J. Katz. *A History of Mathematics: An Introduction*. Addison-Wesley, second edition, November 1998.
- [Koe90] J. J. Koenderink. *Solid Shape*. MIT Press, 1990.
- [Max99] N. Max. Weights for computing vertex normals from facet normals. *Journal of Graphics Tools*, 4(2):1–6, 1999.
- [MD02] J.-L. Maltret and M. Daniel. Discrete curvatures and applications : a survey. Rapport de recherche 004.2002, Laboratoire des Sciences de l’Information et des Systèmes, 2002.
- [MDSB02] M. Meyer, M. Desbrun, P. Schröder, and A. H. Barr. Discrete differential-geometry operators for triangulated 2-manifolds. In *International Workshop on Visualization and Mathematics*, Berlin-Dahlem, Germany, May 2002.
- [MN03] N. J. Mitra and A. Nguyen. Estimating surface normals in noisy point cloud data. In *Symposium on Computational geometry*, pages 322–328. ACM Press, 2003.

- [Mum94] D. Mumford. Elastica and computer vision. In C. L. Bajaj, editor, *Algebraic Geometry and its Applications*, pages 491–506, Springer, 1994.
- [MW00] D. S. Meek and D. J. Walton. On surface normal and gaussian curvature approximations given data sampled from a smooth surface. *Computer Aided Geometric Design*, 17:521–543, 2000.
- [OBS04] Y. Ohtake, A. Belyaev, and H.-P. Seidel. Ridge-valley lines on meshes via implicit surface fitting. *ACM Transactions on Graphics*, 23:609–612, 2004.
- [Pho75] B. T. Phong. Illumination for computer generated pictures. *Communications of ACM*, 18(6):311–317, 1975.
- [Rus04] Szymon Rusinkiewicz. Estimating curvatures and their derivatives on triangle meshes. In *Symposium on 3D Data Processing, Visualization, and Transmission*, pages 486–493. IEEE Computer Society, September 2004.
- [Tau95a] G. Taubin. Estimating the tensor of curvature of a surface from a polyhedral approximation. In *Proc. ICCV'95*, pages 902–907, 1995.
- [Tau95b] Gabriel Taubin. A signal processing approach to fair surface design. In *Proceedings of the 22nd annual conference on Computer graphics and interactive techniques*, pages 351–358. ACM Press, 1995.
- [TRZS04] Holger Theisel, Christian Rössl, Rhaleb Zayer, and Hans-Peter Seidel. Normal based estimation of the curvature tensor for triangular meshes. In *Proceedings of the Computer Graphics and Applications, 12th Pacific Conference on (PG'04)*, pages 288–297. IEEE Computer Society, 2004.
- [WB01] Kouki Watanabe and Alexander G. Belyaev. Detection of salient curvature features on polygonal surfaces. *Comput. Graph. Forum*, 20(3), 2001.

## A Taylor series expansion of space curves

Given an arbitrary curve  $\mathbf{r}(s)$  as in Figure 1 we can analyze it using Taylor series together with the well known Frenet equations [dC76, Koe90]

$$\frac{d\mathbf{t}}{ds} = \kappa\mathbf{n}, \quad \frac{d\mathbf{b}}{ds} = \tau\mathbf{n}, \quad \frac{d\mathbf{n}}{ds} = -\kappa\mathbf{t} - \tau\mathbf{b} \quad (13)$$

where  $\mathbf{t}$ ,  $\mathbf{b}$  and  $\mathbf{n}$  are unit tangent, unit normal and unit binormal vector, respectively, and  $\kappa$  and  $\tau$  are curvature and torsion, respectively. (We omit the position  $s$ , since the equations hold for all (fixed)  $s$  and we are interested only in the case  $s = 0$ , anyway.) Differentiating the curve  $\mathbf{r}(s)$  with respect to its arc length  $s$ , then yields

$$\mathbf{r}' = \mathbf{t}, \quad \mathbf{r}'' = \mathbf{t}' = \kappa\mathbf{n}, \quad \mathbf{r}''' = (\kappa\mathbf{n})' = \kappa'\mathbf{n} - \kappa^2\mathbf{t} - \kappa\tau\mathbf{b}$$

and so on. Now we can use Taylor expansion to express  $\mathbf{e} = \overrightarrow{P_0P_1} = \mathbf{r}(s_1) - \mathbf{r}(s_0)$ :

$$\begin{aligned} \mathbf{e} &= s_1\mathbf{r}' + \frac{s_1^2}{2}\mathbf{r}'' + \frac{s_1^3}{6}\mathbf{r}''' + \frac{s_1^4}{24}\mathbf{r}^{(4)} + \frac{s_1^5}{120}\mathbf{r}^{(5)} + O(s_1^6) \\ &= \mathbf{t}\left(s_1 - \frac{s_1^3}{6}\kappa^2 - \frac{s_1^4}{8}\kappa\kappa' + \frac{s_1^5}{120}(\kappa^4 + \kappa^2\tau^2 - 4\kappa\kappa'' - 3(\kappa')^2) + O(s_1^6)\right) \\ &\quad + \mathbf{n}\left(\frac{s_1^2}{2}\kappa + \frac{s_1^3}{6}\kappa' + \frac{s_1^4}{24}(\kappa'' - \kappa^3 - \kappa\tau^2) - \frac{s_1^5}{120}(6\kappa^2\kappa' + 3\kappa\tau\tau' + 3\kappa'\tau^2 - \kappa^3) + O(s_1^6)\right) \\ &\quad + \mathbf{b}\left(-\frac{s_1^3}{6}\kappa\tau - \frac{s_1^4}{24}(2\kappa'\tau + \kappa\tau') + \frac{s_1^5}{120}(\kappa^3\tau + \kappa\tau^3 - \kappa\tau'' - 3\kappa'\tau' - 3\kappa''\tau) + O(s_1^6)\right). \end{aligned}$$

Since  $(\mathbf{t}, \mathbf{n}, \mathbf{b})$  is an orthonormal basis, we can compute the length  $e$  of  $\mathbf{e}$  in terms of  $s_1$  by

$$e := \|\mathbf{e}\| = s_1 - \frac{s_1^3}{24}\kappa^2 - \frac{s_1^4}{24}\kappa\kappa' + \frac{s_1^5}{5760}(3\kappa^4 + 8\kappa^2\tau^2 - 72\kappa\kappa'' - 64(\kappa')^2) + O(s_1^6).$$

After inverting the Taylor series for  $e$  we obtain

$$s_1 = e + \frac{e^3}{24}\kappa^2 + \frac{e^4}{24}\kappa\kappa' - \frac{e^5}{5760}(3\kappa^4 + 8\kappa^2\tau^2 - 72\kappa\kappa'' - 64(\kappa')^2) + O(e^6).$$

Substituting the expansion of  $s_1$  into the formula for  $\mathbf{e}$  and dividing by  $e$  yields

$$\begin{aligned} \frac{\mathbf{e}}{e} &= \mathbf{t}\left(1 - \frac{e^2}{8}\kappa^2 - \frac{e^3}{12}\kappa\kappa' - \frac{e^4}{1152}(15\kappa^4 - 8\kappa^2\tau^2 + 24\kappa\kappa'' + 16(\kappa')^2) + O(e^5)\right) \\ &\quad + \mathbf{n}\left(\frac{e}{2}\kappa + \frac{e^2}{6}\kappa' + \frac{e^3}{24}(\kappa'' - \kappa\tau^2) + \frac{e^4}{360}(2\kappa^2\kappa' - 9\kappa\tau\tau' - 9\kappa'\tau^2 + 3\kappa''') + O(e^5)\right) \\ &\quad + \mathbf{b}\left(-\frac{e^2}{6}\kappa\tau - \frac{e^3}{24}(2\kappa'\tau + \kappa\tau') \right. \\ &\quad \quad \left. - \frac{e^4}{360}(2\kappa^3\tau - 3\kappa\tau^3 + 3\kappa\tau'' + 9\kappa'\tau' + 9\kappa''\tau) + O(e^5)\right). \end{aligned}$$

In the same way we get the expressions for  $\frac{\mathbf{d}}{d}$ ,  $\frac{\mathbf{e}}{c}$  and  $\frac{\mathbf{f}}{f}$ :

$$\begin{aligned}\frac{\mathbf{d}}{d} &= \mathbf{t}\left(1 - \frac{d^2}{8}\kappa^2 + \frac{d^3}{12}\kappa\kappa' + O(d^4)\right) \\ &+ \mathbf{n}\left(-\frac{d}{2}\kappa + \frac{d^2}{6}\kappa' - \frac{d^3}{24}(\kappa'' - \kappa\tau^2) + O(d^4)\right) \\ &+ \mathbf{b}\left(-\frac{d^2}{6}\kappa\tau + \frac{d^3}{24}(2\kappa'\tau + \kappa\tau') + O(d^4)\right), \\ \frac{\mathbf{c}}{c} &= \mathbf{t}\left(1 - \frac{c^2 + 4cd + 4d^2}{8}\kappa^2 + \frac{c^3 + 5c^2d + 9cd^2 + 6d^3}{12}\kappa\kappa' + O(c, d^4)\right) \\ &+ \mathbf{n}\left(-\frac{c + 2d}{2}\kappa + \frac{c^2 + 3cd + 3d^2}{6}\kappa' + \frac{c^2d + 2cd^2 + d^3}{8}\kappa^3 \right. \\ &\quad \left. - \frac{c^3 + 4c^2d + 6cd^2 + 4d^3}{24}(\kappa'' - \kappa\tau^2) + O(c, d^4)\right) \\ &+ \mathbf{b}\left(-\frac{c^2 + 3cd + 3d^2}{6}\kappa\tau + \frac{c^3 + 4c^2d + 6cd^2 + 4d^3}{24}(2\kappa'\tau + \kappa\tau') + O(c, d^4)\right),\end{aligned}$$

and

$$\begin{aligned}\frac{\mathbf{f}}{f} &= \mathbf{t}\left(1 - \frac{f^2 + 4fe + 4e^2}{8}\kappa^2 - \frac{f^3 + 5f^2e + 9fe^2 + 6e^3}{12}\kappa\kappa' + O(e, f^4)\right) \\ &+ \mathbf{n}\left(\frac{f + 2e}{2}\kappa + \frac{f^2 + 3fe + 3e^2}{6}\kappa' - \frac{f^2e + 2fe^2 + e^3}{8}\kappa^3 \right. \\ &\quad \left. + \frac{f^3 + 4f^2e + 6fe^2 + 4e^3}{24}(\kappa'' - \kappa\tau^2) + O(e, f^4)\right) \\ &+ \mathbf{b}\left(-\frac{f^2 + 3fe + 3e^2}{6}\kappa\tau - \frac{f^3 + 4f^2e + 6fe^2 + 4e^3}{24}(2\kappa'\tau + \kappa\tau') + O(e, f^4)\right).\end{aligned}$$

Using the above expansions we can also compute the cross product of  $\frac{\mathbf{d}}{d}$  and  $\frac{\mathbf{e}}{e}$ :

$$\begin{aligned}\frac{\mathbf{d}}{d} \times \frac{\mathbf{e}}{e} &= \mathbf{t}\left(\frac{d^2e + de^2}{12}\kappa^2\tau + O(d, e^4)\right) \\ &+ \mathbf{n}\left(\frac{e^2 - d^2}{6}\kappa\tau + \frac{d^3 + e^3}{24}(2\kappa'\tau + \kappa\tau') + O(d, e^4)\right) \\ &+ \mathbf{b}\left(\frac{d + e}{2}\kappa + \frac{e^2 - d^2}{6}\kappa' + \frac{d^3 + e^3}{24}(\kappa'' - \kappa\tau^2) - \frac{d^2e + de^2}{16}\kappa^3 + O(d, e^4)\right).\end{aligned}$$

Note that the quadratic terms vanish for  $d = e$ . The same is true for fourth order

terms:

$$\begin{aligned} \frac{\mathbf{d}}{d} \times \frac{\mathbf{e}}{e} &\stackrel{d=e}{=} \mathbf{t} \left( \frac{e^3}{6} \kappa^2 \tau + O(e^5) \right) \\ &+ \mathbf{n} \left( \frac{e^3}{12} (2\kappa' \tau + \kappa \tau') + O(e^5) \right) \\ &+ \mathbf{b} \left( e\kappa + \frac{e^3}{12} (\kappa'' - \kappa \tau^2) - \frac{e^3}{8} \kappa^3 + O(e^5) \right). \end{aligned}$$

Since the norm of the above vector equals  $\sin \varphi$  we obtain

$$\begin{aligned} \sin \varphi &= \frac{d+e}{2} \kappa - \frac{d^2-e^2}{6} \kappa' + \frac{(d-e)(d^2-e^2)}{36} \kappa \tau^2 \\ &+ \frac{d^3+e^3}{24} (\kappa'' - \kappa \tau^2) - \frac{d^2e+de^2}{16} \kappa^3 + O(d, e)^4, \\ \varphi &= \frac{d+e}{2} \kappa - \frac{d^2-e^2}{6} \kappa' + \frac{d^3+e^3}{48} (\kappa^3 - \frac{2}{3} \kappa \tau^2 + 2\kappa'') \\ &- \frac{d^2e+de^2}{36} \kappa \tau^2 + O(d, e)^4, \end{aligned}$$

and for  $d = e$

$$\varphi \stackrel{d=e}{=} e\kappa + \frac{e^3}{24} (2\kappa'' + \kappa^3 - 2\kappa \tau^2) + O(e^5).$$

We can also compute the normalized binormal at  $P_0$  by

$$\begin{aligned} \mathbf{b}_0 &:= \frac{\mathbf{d} \times \mathbf{e}}{\|\mathbf{d} \times \mathbf{e}\|} = \frac{\frac{\mathbf{d}}{d} \times \frac{\mathbf{e}}{e}}{\sin \varphi} \\ &= \mathbf{t} \left( \frac{de}{6} \kappa \tau + O(d, e)^3 \right) \\ &+ \mathbf{n} \left( \frac{e-d}{3} \tau + \frac{d^2-de+e^2}{12} \tau' + \frac{d^2+de+e^2}{18} \frac{\kappa'}{\kappa} \tau + O(d, e)^3 \right) \\ &+ \mathbf{b} \left( 1 - \frac{(d-e)^2}{18} \tau^2 + O(d, e)^3 \right). \end{aligned}$$

The terms for the binormals  $\mathbf{b}_{-1}$  at  $P_{-1}$  and  $\mathbf{b}_1$  at  $P_1$  are similar:

$$\begin{aligned} \mathbf{b}_{-1} &:= \frac{\mathbf{c} \times \mathbf{d}}{\|\mathbf{c} \times \mathbf{d}\|} \\ &= \mathbf{t} \left( -\frac{cd+d^2}{6} \kappa \tau + O(c, d)^3 \right) \\ &+ \mathbf{n} \left( -\frac{c+2d}{3} \tau + \frac{c^2+3cd+3d^2}{12} \tau' + \frac{c^2+cd+d^2}{18} \frac{\kappa'}{\kappa} \tau + O(c, d)^3 \right) \\ &+ \mathbf{b} \left( 1 - \frac{c^2+4cd+4d^2}{18} \tau^2 + O(c, d)^3 \right) \end{aligned}$$

and

$$\begin{aligned}
\mathbf{b}_1 &:= \frac{\mathbf{e} \times \mathbf{f}}{\|\mathbf{e} \times \mathbf{f}\|} \\
&= \mathbf{t} \left( -\frac{fe + e^2}{6} \kappa \tau + O(e, f)^3 \right) \\
&\quad + \mathbf{n} \left( \frac{f + 2e}{3} \tau + \frac{f^2 + 3fe + 3e^2}{12} \tau' + \frac{f^2 + fe + e^2}{18} \frac{\kappa'}{\kappa} \tau + O(e, f)^3 \right) \\
&\quad + \mathbf{b} \left( 1 - \frac{f^2 + 4fe + 4e^2}{18} \tau^2 + O(e, f)^3 \right).
\end{aligned}$$

With those we can in turn estimate the angle between two consecutive binormals as

$$\begin{aligned}
\hat{\eta} = \langle \mathbf{b}_1 \times \mathbf{b}_0, \tilde{\mathbf{t}} \rangle &= \frac{d + e + f}{3} \tau - \frac{d^2 + de - ef - f^2}{18} \frac{\kappa'}{\kappa} \tau \\
&\quad - \frac{d^2 - de - 2e^2 - 3ef - f^2}{12} \tau' + O(d, e, f)^3
\end{aligned}$$

where  $\tilde{\mathbf{t}}$  is the tangent approximation from equation (6).

## B Taylor series expansion of geodesics

The behavior of the Darboux frame for an arbitrary smooth curve  $\mathbf{r}(s)$  on a surface  $\mathcal{S}$  is governed by the following modified Frenet-Serret equations [dC76, Koe90]

$$\begin{pmatrix} d\mathbf{t}/ds \\ d\mathbf{v}/ds \\ d\mathbf{n}/ds \end{pmatrix} = \begin{pmatrix} 0 & \kappa_g & \kappa_n \\ -\kappa_g & 0 & \tau \\ -\kappa_n & -\tau & 0 \end{pmatrix} \begin{pmatrix} \mathbf{t} \\ \mathbf{v} \\ \mathbf{n} \end{pmatrix}$$

where  $\kappa_n$  is the normal curvature,  $\kappa_g$  is the geodesic curvature, and  $\tau$  is the geodesic torsion of the curve. Thus for the geodesic  $\mathbf{g}_i(s)$  as defined in Section 3 we have

$$\frac{d\mathbf{t}_i}{ds} = \kappa_i \mathbf{n}, \quad \frac{d\mathbf{v}_i}{ds} = \tau_i \mathbf{n}, \quad \frac{d\mathbf{n}}{ds} = -\kappa_i \mathbf{t}_i - \tau_i \mathbf{v}_i,$$

where  $\kappa_i(s)$  and  $\tau_i(s)$  are the normal curvature and geodesic torsion of  $\mathbf{g}_i(s)$ , respectively. Note that these are exactly the same equations as for the space curves given in equation (13), only with a slightly different meaning of  $\kappa_i$  and  $\tau_i$  compared to  $\kappa$  and  $\tau$ . Therefore, we have (formally) exactly the same Taylor series expansions for  $\mathbf{a}_i := \overrightarrow{PQ}_i$  and  $a_i := \|\mathbf{a}_i\|$  as for  $\mathbf{e}$  and  $e$  in Appendix A and get finally

$$\frac{\mathbf{a}_i}{a_i} = \mathbf{t}_i \left( 1 - \frac{a_i^2}{8} \kappa_i^2 + O(a_i^3) \right) + \mathbf{v}_i \left( -\frac{a_i^2}{6} \kappa_i \tau_i + O(a_i^3) \right) + \mathbf{n} \left( \frac{a_i}{2} \kappa_i + \frac{a_i^2}{6} \kappa_i' + O(a_i^3) \right).$$

Let  $\beta_i$  be the angle between  $\mathbf{t}_i$  and  $\mathbf{t}_{i+1}$  (indices taken modulo  $n$ ), see Figure 8 on the right hand side. Now we can compute the normal of an incident triangle at  $P$  as

$$\begin{aligned}
\frac{\mathbf{a}_i}{a_i} \times \frac{\mathbf{a}_{i+1}}{a_{i+1}} &= \sin \beta_i \mathbf{n} \left( 1 - \frac{a_i^2}{8} \kappa_i^2 - \frac{a_{i+1}^2}{8} \kappa_{i+1}^2 + O(a_i, a_{i+1})^3 \right) \\
&\quad + \cos \beta_i \mathbf{n} \left( -\frac{a_{i+1}^2}{6} \kappa_{i+1} \tau_{i+1} + O(a_i, a_{i+1})^3 \right) \\
&\quad - \mathbf{v}_i \left( \frac{a_{i+1}}{2} \kappa_{i+1} + \frac{a_{i+1}^2}{6} \kappa'_{i+1} + O(a_i, a_{i+1})^3 \right) \\
&\quad - \cos \beta_i \mathbf{n} \left( -\frac{a_i^2}{6} \kappa_i \tau_i + O(a_i, a_{i+1})^3 \right) \\
&\quad + \sin \beta_i \mathbf{n} \left( O(a_i, a_{i+1})^3 \right) \\
&\quad + \mathbf{t}_i \left( O(a_i, a_{i+1})^3 \right) \\
&\quad + \mathbf{v}_{i+1} \left( \frac{a_i}{2} \kappa_i + \frac{a_i^2}{6} \kappa'_i + O(a_i, a_{i+1})^3 \right) \\
&\quad - \mathbf{t}_{i+1} \left( O(a_i, a_{i+1})^3 \right).
\end{aligned}$$

Since  $\beta_i$  equals the angle  $\alpha_i$  between  $\mathbf{a}_i$  and  $\mathbf{a}_{i+1}$  up to quadratic order we can also use that angle in our asymptotic formula (compare also [MD02]):

$$\begin{aligned}
\sin \alpha_i = \left\| \frac{\mathbf{a}_i}{a_i} \times \frac{\mathbf{a}_{i+1}}{a_{i+1}} \right\| &= \sin \beta_i + \left( \frac{1}{\sin \beta_i} - \sin \beta_i \right) \left( \frac{a_i^2}{8} \kappa_i^2 + \frac{a_{i+1}^2}{8} \kappa_{i+1}^2 \right) \\
&\quad + \cos \beta_i \left( \frac{a_i^2}{6} \kappa_i \tau_i - \frac{a_{i+1}^2}{6} \kappa_{i+1} \tau_{i+1} \right) - \cot \beta_i \left( \frac{a_i a_{i+1}}{4} \kappa_i \kappa_{i+1} \right) + O(a_i, a_{i+1})^3
\end{aligned}$$

and therefore  $\alpha_i = \beta_i + O(a_i, a_{i+1})^2$ .

But we can also use this result to compute  $\frac{\mathbf{a}_i \times \mathbf{a}_{i+1}}{\|\mathbf{a}_i \times \mathbf{a}_{i+1}\|}$ . Now suppose  $a_i = a_{i+m}$  and  $\alpha_i = \alpha_{i+m}$ . We know

$$2 \sum_{j=i}^{i+m-1} \alpha_j = \sum_{j=1}^{2m} \alpha_j = \sum_{j=1}^{2m} \beta_j + O(a_j)^2 = 2\pi + O(a_j)^2.$$

Therefore, we get

$$\beta_{i,i+m} = \sum_{j=i}^{i+m-1} \beta_j = \sum_{j=i}^{i+m-1} \alpha_j + O(a_j)^2 = \pi + O(a_j)^2,$$

$$\mathbf{v}_{i+m} = \cos \beta_{i,i+m-1} \mathbf{v}_i - \sin \beta_{i,i+m-1}, \quad \mathbf{t}_i = -\mathbf{v}_i (1 + O(a_j)^2) + \mathbf{t}_i (O(a_j)^2),$$

and the corresponding result for  $\mathbf{t}_{i+m}$  where  $\beta_{ij}$  is the counter-clockwise angle between  $\mathbf{t}_i$  and  $\mathbf{t}_j$ . Using Euler's formula

$$\kappa_i = \kappa_{\max} \cos^2 \theta + \kappa_{\min} \sin^2 \theta$$

for curvature and the corresponding

$$\tau_i = (\kappa_{\max} - \kappa_{\min}) \cos \theta \sin \theta$$

for torsion we obtain

$$\kappa_{i+m} = \kappa_i + O(a_j)^2 \quad \text{and} \quad \tau_{i+m} = \tau_i + O(a_j)^2.$$

We can also use our computations to gain an estimation of the angular error. We compute the scalar product to obtain the cosine of the angle

$$\begin{aligned} & \left\langle \frac{\mathbf{a}_i \times \mathbf{a}_{i+1}}{\|\mathbf{a}_i \times \mathbf{a}_{i+1}\|}, \mathbf{n} \right\rangle \\ &= 1 - \frac{1}{8 \sin^2 \alpha_i} (a_i^2 \kappa_i^2 + a_{i+1}^2 \kappa_{i+1}^2 - 2a_i a_{i+1} \kappa_i \kappa_{i+1} \cos \alpha_i) + O(a_i, a_{i+1})^3. \end{aligned}$$

Therefore, the angular error has to be

$$\frac{1}{2 \sin \alpha_i} \cdot \sqrt{a_i^2 \kappa_i^2 + a_{i+1}^2 \kappa_{i+1}^2 - 2a_i a_{i+1} \kappa_i \kappa_{i+1} \cos \alpha_i} + O(a_i, a_{i+1})^2.$$

Because the curvature is unknown anyway we simplify the term by setting  $\kappa_i = \kappa_{i+1} = 1$  and we get

$$\frac{1}{2 \sin \alpha_i} \sqrt{a_i^2 + a_{i+1}^2 - 2a_i a_{i+1} \cos \alpha_i}$$

as the main error term. We note that the square root equals the length of the edge  $\mathbf{d}_i$  opposing  $P$ , see Figure 2.

This justifies to use  $\frac{\sin \alpha_i}{d_i}$  as weights for the unit facet normals  $\mathbf{n}_i$  of a one-ring. It uses the inverse of the estimated angular error to give stronger weights to triangles whose normals are closer to the real normal.

## C Euler's elastica for space curves

In this section we will derive necessary conditions for a space curve  $\mathbf{r}(s)$  to be an elastica, i. e.

$$\int \kappa^2 ds \longrightarrow \min,$$

while fixing position and tangent of the two end points. Hereby we follow the treatment given in [BAYY99] and [Mum94] for elastica in the plane.

We consider a small perturbation of  $\mathbf{r}(s)$

$$\hat{\mathbf{r}}(s) := \mathbf{r}(s) + \epsilon(h(s)\mathbf{n} + k(s)\mathbf{b})$$

where  $\mathbf{r}(s)$  is an elastica parameterized by arc length  $s$ ,  $h(s)$  and  $k(s)$  are real functions with compact support and  $\epsilon$  is a real number. Using the Frenet equations we get

$$\frac{d\hat{\mathbf{r}}}{ds} = \mathbf{t} + \epsilon(-h\kappa\mathbf{t} + (h' + k\tau)\mathbf{n} + (k' - h\tau)\mathbf{b}).$$

Let  $\hat{\mathbf{r}}(\hat{s})$  be a parameterization of  $\hat{\mathbf{r}}$  by arc length. Then

$$d\hat{s} = \left\| \frac{d\hat{\mathbf{r}}}{ds} \right\| ds = (1 - \epsilon h\kappa + O(\epsilon^2)) ds.$$

Therefore, we have

$$\begin{aligned} \hat{\mathbf{t}} &= \frac{d\hat{\mathbf{r}}}{d\hat{s}} = \frac{d\hat{\mathbf{r}}}{ds} \frac{ds}{d\hat{s}} = \mathbf{t} + \epsilon((h' + k\tau)\mathbf{n} + (k' - h\tau)\mathbf{b}) + O(\epsilon^2), \\ \hat{\kappa}\hat{\mathbf{n}} &= \frac{d\hat{\mathbf{t}}}{d\hat{s}} = \frac{d\hat{\mathbf{t}}}{ds} \frac{ds}{d\hat{s}} \\ &= \kappa\mathbf{n} + \epsilon(-h'\kappa - k\kappa\tau) \\ &\quad + \epsilon(h(\kappa^2 - \tau^2) + h'' + k\tau' + 2k'\tau)\mathbf{n} + \epsilon(-h\tau' - 2h'\tau - k\tau^2 + k'')\mathbf{b} + O(\epsilon^2) \end{aligned}$$

and

$$\hat{\kappa}^2 = \|\hat{\kappa}\hat{\mathbf{n}}\|^2 = \kappa^2 + 2\epsilon\kappa(h(\kappa^2 - \tau^2) + h'' + k\tau' + 2k'\tau) + O(\epsilon^2).$$

Now we can compute, using integration by parts:

$$\int \hat{\kappa}^2 d\hat{s} = \int \kappa^2 ds + \epsilon \int h(\kappa^3 + 2\kappa'' - 2\kappa\tau^2) - 2k(\kappa\tau' + 2\kappa'\tau) ds + O(\epsilon^2).$$

Because  $h(s)$  and  $k(s)$  are arbitrary functions with compact support and the integral  $\int \kappa^2 ds$  is minimal for  $\mathbf{r}(s)$ , this shows:

$$\kappa'' + \frac{\kappa^3}{2} - \kappa\tau^2 = 0 \quad \text{and} \quad \kappa'\tau + \frac{\kappa\tau'}{2} = 0.$$



Below you find a list of the most recent technical reports of the Max-Planck-Institut für Informatik. They are available by anonymous ftp from [ftp.mpi-sb.mpg.de](ftp://ftp.mpi-sb.mpg.de) under the directory `pub/papers/reports`. Most of the reports are also accessible via WWW using the URL <http://www.mpi-sb.mpg.de>. If you have any questions concerning ftp or WWW access, please contact [reports@mpi-sb.mpg.de](mailto:reports@mpi-sb.mpg.de). Paper copies (which are not necessarily free of charge) can be ordered either by regular mail or by e-mail at the address below.

Max-Planck-Institut für Informatik  
Library  
attn. Anja Becker  
Stuhlsatzenhausweg 85  
66123 Saarbrücken  
GERMANY  
e-mail: [library@mpi-sb.mpg.de](mailto:library@mpi-sb.mpg.de)

---

MPI-I-2005-4-004	C. Theobalt, N. Ahmed, E. De Aguiar, G. Ziegler, H. Lensch, M.A., Magnor, H. Seidel	Joint Motion and Reflectance Capture for Creating Relightable 3D Videos
MPI-I-2005-4-003	T. Langer, A.G. Belyaev, H. Seidel	Analysis and Design of Discrete Normals and Curvatures
MPI-I-2005-4-002	O. Schall, A. Belyaev, H. Seidel	Sparse Meshing of Uncertain and Noisy Surface Scattered Data
MPI-I-2005-4-001	M. Fuchs, V. Blanz, H. Lensch, H. Seidel	Reflectance from Images: A Model-Based Approach for Human Faces
MPI-I-2005-2-001	J. Hoffmann, Carla Gomes	Bottleneck Behavior in CNF Formulas
MPI-I-2005-1-002	I. Katriel, M. Kutz, M. Skutella	Reachability Substitutes for Planar Digraphs
MPI-I-2005-1-001	D. Michail	Rank-Maximal through Maximum Weight Matchings
MPI-I-2004-NWG3-001	M. Magnor	Axisymmetric Reconstruction and 3D Visualization of Bipolar Planetary Nebulae
MPI-I-2004-NWG1-001	B. Blanchet	Automatic Proof of Strong Secrecy for Security Protocols
MPI-I-2004-5-001	S. Siersdorfer, S. Sizov, G. Weikum	Goal-oriented Methods and Meta Methods for Document Classification and their Parameter Tuning
MPI-I-2004-4-006	K. Dmitriev, V. Havran, H. Seidel	Faster Ray Tracing with SIMD Shaft Culling
MPI-I-2004-4-005	I.P. Ivrişimţizis, W.-. Jeong, S. Lee, Y.a. Lee, H.-. Seidel	Neural Meshes: Surface Reconstruction with a Learning Algorithm
MPI-I-2004-4-004	R. Zayer, C. Rssl, H. Seidel	r-Adaptive Parameterization of Surfaces
MPI-I-2004-4-003	Y. Ohtake, A. Belyaev, H. Seidel	3D Scattered Data Interpolation and Approximation with Multilevel Compactly Supported RBFs
MPI-I-2004-4-002	Y. Ohtake, A. Belyaev, H. Seidel	Quadric-Based Mesh Reconstruction from Scattered Data
MPI-I-2004-4-001	J. Haber, C. Schmitt, M. Koster, H. Seidel	Modeling Hair using a Wisp Hair Model
MPI-I-2004-2-002	P. Maier	Intuitionistic LTL and a New Characterization of Safety and Liveness
MPI-I-2004-2-001	H.d. Nivelle, Y. Kazakov	Resolution Decision Procedures for the Guarded Fragment with Transitive Guards
MPI-I-2004-1-007	S. Wagner	Summaries for While Programs with Recursion
MPI-I-2004-1-006	L.S. Chandran, N. Sivasadan	On the Hadwiger's Conjecture for Graph Products
MPI-I-2004-1-005	S. Schmitt, L. Fousse	A comparison of polynomial evaluation schemes
MPI-I-2004-1-004	N. Sivasadan, P. Sanders, M. Skutella	Online Scheduling with Bounded Migration
MPI-I-2004-1-003	I. Katriel	On Algorithms for Online Topological Ordering and Sorting
MPI-I-2004-1-002	P. Sanders, S. Pettie	A Simpler Linear Time $2/3$ - epsilon Approximation for Maximum Weight Matching

MPI-I-2004-1-001	N. Beldiceanu, I. Katriel, S. Thiel	Filtering algorithms for the Same and UsedBy constraints
MPI-I-2003-NWG2-002	F. Eisenbrand	Fast integer programming in fixed dimension
MPI-I-2003-NWG2-001	L.S. Chandran, C.R. Subramanian	Girth and Treewidth
MPI-I-2003-4-009	N. Zakaria	FaceSketch: An Interface for Sketching and Coloring Cartoon Faces
MPI-I-2003-4-008	C. Roessl, I. Ivriissimtzis, H. Seidel	Tree-based triangle mesh connectivity encoding
MPI-I-2003-4-007	I. Ivriissimtzis, W. Jeong, H. Seidel	Neural Meshes: Statistical Learning Methods in Surface Reconstruction
MPI-I-2003-4-006	C. Roessl, F. Zeilfelder, G. Nrnberger, H. Seidel	Visualization of Volume Data with Quadratic Super Splines
MPI-I-2003-4-005	T. Hangelbroek, G. Nrnberger, C. Roessl, H.S. Seidel, F. Zeilfelder	The Dimension of $C^1$ Splines of Arbitrary Degree on a Tetrahedral Partition
MPI-I-2003-4-004	P. Bekaert, P. Slusallek, R. Cools, V. Havran, H. Seidel	A custom designed density estimation method for light transport
MPI-I-2003-4-003	R. Zayer, C. Roessl, H. Seidel	Convex Boundary Angle Based Flattening
MPI-I-2003-4-002	C. Theobalt, M. Li, M. Magnor, H. Seidel	A Flexible and Versatile Studio for Synchronized Multi-view Video Recording
MPI-I-2003-4-001	M. Tarini, H.P.A. Lensch, M. Goesele, H. Seidel	3D Acquisition of Mirroring Objects
MPI-I-2003-2-004	A. Podelski, A. Rybalchenko	Software Model Checking of Liveness Properties via Transition Invariants
MPI-I-2003-2-003	Y. Kazakov, H. Nivelte	Subsumption of concepts in $DL\mathcal{FL}_0$ for (cyclic) terminologies with respect to descriptive semantics is PSPACE-complete
MPI-I-2003-2-002	M. Jaeger	A Representation Theorem and Applications to Measure Selection and Noninformative Priors
MPI-I-2003-2-001	P. Maier	Compositional Circular Assume-Guarantee Rules Cannot Be Sound And Complete
MPI-I-2003-1-018	G. Schaefer	A Note on the Smoothed Complexity of the Single-Source Shortest Path Problem
MPI-I-2003-1-017	G. Schfer, S. Leonardi	Cross-Monotonic Cost Sharing Methods for Connected Facility Location Games
MPI-I-2003-1-016	G. Schfer, N. Sivadasan	Topology Matters: Smoothed Competitive Analysis of Metrical Task Systems
MPI-I-2003-1-015	A. Kovcs	Sum-Multicoloring on Paths
MPI-I-2003-1-014	G. Schfer, L. Becchetti, S. Leonardi, A. Marchetti-Spaccamela, T. Vredeveld	Average Case and Smoothed Competitive Analysis of the Multi-Level Feedback Algorithm
MPI-I-2003-1-013	I. Katriel, S. Thiel	Fast Bound Consistency for the Global Cardinality Constraint
MPI-I-2003-1-012		- not published -
MPI-I-2003-1-011	P. Krysta, A. Czumaj, B. Voecking	Selfish Traffic Allocation for Server Farms
MPI-I-2003-1-010	H. Tamaki	A linear time heuristic for the branch-decomposition of planar graphs
MPI-I-2003-1-009	B. Csaba	On the Bollobás – Eldridge conjecture for bipartite graphs
MPI-I-2003-1-008	P. Sanders	Polynomial Time Algorithms for Network Information Flow
MPI-I-2003-1-007	H. Tamaki	Alternating cycles contribution: a strategy of tour-merging for the traveling salesman problem
MPI-I-2003-1-006	M. Dietzfelbinger, H. Tamaki	On the probability of rendezvous in graphs
MPI-I-2003-1-005	M. Dietzfelbinger, P. Woelfel	Almost Random Graphs with Simple Hash Functions
MPI-I-2003-1-004	E. Althaus, T. Polzin, S.V. Daneshmand	Improving Linear Programming Approaches for the Steiner Tree Problem